Comparative Studies of Zn Alloys using LIBS and EDX Techniques

By

Muhammad Sajid

Department of Physics

Quaid-i-Azam University

Islamabad, Pakistan

June, 2016

This work is submitted as a dissertation in partial fulfilment of the requirement for the degree of

Master of philosophy

in

PHYSICS

Department of Physics

Quaid-i-Azam University

Islamabad, Pakistan

June, 2016

CERTIFICATE

It is certified that the work contained in this thesis is carried out and completed under my supervision at the Atomic and Molecular Physics, Laboratory, Department of Physics, Quaid-i-Azam University, Islamabad, Pakistan.

Supervisor

Prof. Dr. M Aslam Baig (H.I, T.I, S.I)

Distinguished National Professor
National Centre of Physics
Quaid-i-Azam university campus, Islamabad

Submitted through

Prof. Dr. Khalid Khan

(Chairman)

Department of Physics
Quaid-i-Azam University, Islamabad.

Dedicated to

My Parents

And Spouse

ACKNOWLEDGMENT

It would be impossible for me to stand where I am without the assistance of my supervisor and teachers. I want to express my extreme gratitude for my supervisor Prof. Dr. M. Aslam Baig (S.I, H.I, T.I) for his keen interest and kind supervision. Additionally, I also feel obliged to thank Dr. Rizwan Ahmed for his continuous guidance and help during my whole research work.

I also like to thank my NCP Lab fellows especially Javaid Iqbal and Nasar Ahmed for their assistance. Inspiration and motivation of Dr. Zeshan Adeel Umar made it easy for me to complete my work effectively and superbly.

Moreover, I am thankful to my colleagues at Quaid I Azam University especially Mr. Naveed and Mr. Rafaqat Riaz who helped me to do experiment and guided me to the best of their knowledge.

Last but not the least, I am very grateful to my parents and siblings who supported and encouraged me at each step of my life.

Muhammad Sajid

Contents

List of Figures

Chapter No. 2

Chapter No. 4

List of Tables

Abstract

Laser induced breakdown spectroscopy (LIBS) has been used to study the laser induced plasma of Zinc and Aluminium. Five samples of Zinc with varying concentration of Aluminium were prepared by mixing pure powders and pressing it under great pressures to form pallets. Q-switched Nd:YAG laser has been used for ablation and Avantes spectrometer was used to record emission spectrum of ablated plasma covering the range of 250nm to 900nm. In the present work, calibration curve (CC-LIBS) and calibration free LIBS (CF-LIBS) techniques have been used for quantitatively analyse the samples. One line calibration curve is used in CF-LIBS. For the quantitative analysis using LIBS technique, the ablated plasma must be optically thin and fulfil the condition of local thermodynamic equilibrium condition. Temperature of ablated plasma was determined by the slope of Boltzmann plots and electron number density was determined by measuring Stark broadening for Al peak. Quantitative Analysis of the sample was also carried out using more standard techniques i.e. EDX and XRF for comparison. At the end, it is concluded that calibration curve method is much accurate than calibration free LIBS technique which still require more research to be carried out on it.

Chapter No. 1

Introduction

This chapter includes the fundamentals, types, operations and applications of laser, introduction and basic techniques of atomic spectroscopy, introduction, applications, basic parameters of laser induced breakdown spectroscopy (LIBS), methods to calculate the plasma temperature and electron number density and the factors affecting the plasma temperature. Aim of our work which is the quantitative analysis by LIBS and its comparison with other techniques i.e. EDX and XRF, described at the end of this chapter.

1 Laser

1.1 Introduction of Laser

Laser (Light Amplification through Stimulated Emission of Radiation) is a mechanism by which intense, monochromatic and coherent beam of light can be produced. Its wavelength ranges from UV down to microwave (often known as MASER) and average power ranges from 1 mW to 3000 W. Due to its directionality and mono-chromaticity, it has vast applications in almost every field. [1, 2]

1.2 History of Laser

On the basis of quantum theory of radiation, *Albert Einstein*, in 1917, presented the theory of laser and proved that coherent and monochromatic beam of light can be produced by stimulated emission. After that, Charles Townes and Arthur Schawlow completed the theoretical work for laser and first laser came into existence in 1960 by Theodore Maiman. It was a solid state Ruby laser. [3, 4] Nd:YAG laser is also a solid state laser which came into existence around 1964. [5]

1.3 The Basic Principle

Laser is based on the concept of stimulated emission. A photon of energy equal to the energy difference of the energy levels causes the excited atom to de-excite instantly and produce a coherent photon of same energy. So, number of existing photons gets doubled. These photons triggers more stimulated emission processes. By moving photons to and fro in an optical resonator, avalanche process occurs and number of photons gets increased many times. One of the important pre-requisite for the Laser to occur is population inversion. Under normal conditions, there are more ground state atoms than excited state ones in a cavity. For the Laser to sustain, population of excited state must be more than that of lower state. This non equilibrium thermal state is population inversion. To sustain such a state, energy must be

constantly pumped in the system either by optically pumping the atoms with some light source or electrical pumping by electric discharge. Optical pumping is used in solid state lasers (Nd:YAG) while electrical pumping is used in gas lasers like He-Ne laser. Pumping ensures the population inversion to sustain.

In order for laser to function, the active medium must have a metastable state. Metastable states are those states which cannot decay via spontaneous emission. Lifetime of these states is many orders of magnitude more than the lifetime of usual excited states. This peculiar nature of these states is exploited to make laser.

Laser has vast applications in every field which also include spectroscopic techniques. A mono chromatic, intense beam is capable to produce atomic transitions which are, in turn, signature of peculiar atoms.

2 Spectroscopy

Spectroscopy is by far only technique by which one can get knowledge about a sample. Every atom or molecule has its well-defined energy levels for electron to occupy. A photon of characteristic wavelength and energy is emitted or absorbed whenever an electron makes a transition from one level to another. Since every atomic or molecular specie has distinct energy states, they can be used to get composition of any sample. By resolution of spectrum, sample can be analyzed qualitatively and quantitatively. Different techniques differ in their modes of exciting electrons e.g. electric discharge, laser or x-rays etc. or detection methods. Three techniques are usually applied in this field:

2.1 Atomic Emission Spectroscopy (AES)

In AES, energy is given to the sample by either electric discharge or by electromagnetic radiation. Atoms absorb this energy and its electrons jumps up to higher energy levels. These excited states cannot remain indefinitely; rather they decay to ground levels emitting photons of energy equal to energy difference of levels. These excited levels, upon de-excitation, give off light of characteristic wavelength. By measuring their wavelength and intensity, detection and concentration of individual elements is obtained.

2.2 Atomic Absorption Spectroscopy (AAS)

In AAS, electromagnetic radiation of mixture of wavelengths is allowed to fall on the sample. Atoms in the sample only absorb the wavelengths associated with its energy levels. As the absorption is proportional to the number of atoms in the sample, diminished intensity is used for elemental analysis.

2.3 Atomic Mass Spectrometry (AMS)

In AMS, atoms are first ionized and then moved by a pre-set electric field. These ions reach the other electrode at different times owing to their charge to mass ratio and produce tiny currents. It can also be used to separate ions. Even isotopes of same elements can be separated and their relative abundances can be calculated.

3 Introduction to Laser Induced Breakdown Spectroscopy (LIBS)

LIBS acronym for Laser Induced Breakdown Spectroscopy is a technique to carry out elemental analysis of material. It is a type of atomic emission spectroscopy. It is better than other similar techniques in the sense that it is fast and low cost. Furthermore, it has the ability to detect virtually all the elements of periodic table and find out their elemental compositions qualitatively as well as quantitatively. Portable spectroscopic machines are also available. By using LIBS, qualitative as well as quantitative analysis of sample can be carried out. It has been widely in use for the analysis of metals, non-metals and other liquid and gaseous samples [41, 42]. It is also used to check food items like different vegetables [43] and dry fruits [44].

3.1 Basic Principle of LIBS

When high power pulse of laser is targeted over a sample, breakdown takes place at the spot making excited states of neutral as well as ionized species. [7, 37, 38] This ablated plasma cools down quickly giving photons of characteristic transitions. A spectrometer is installed which collects the emitted light and with the help of computer, produce a wavelength dispersive spectrum. The intensities of individual lines help us to identify and carry out the quantitative analysis of the sample.

3.2 Characteristics of Plasma

Just after the laser strike, matter ablates to form ionized species of each element, usually referred as plasma with a condition that, any ionized gas can be called as plasma if it ion number density satisfies: [9]

$$N_D = \frac{4\pi}{3}(\lambda_D)^3 n_0 \geq 1 \qquad (1.1)$$

N_D is the number of ions present in the sphere of radius equal to Debye length, which is, in turn, equal to:

$$\lambda_D = \left(\frac{\epsilon_0 k_\beta T_e}{e^2 n_0}\right)^{1/2} \qquad (1.2)$$

n_0 is number density of electrons and ion pairs, λ_D is the Debye length which should be much smaller than plasma dimensions. ϵ_0 is permittivity of free space, T_e is electron temperature and k_β is Boltzmann constant. A plasma shield is formed which resists the pulse

to reach the sample and plasma spreads towards the laser pulse making a shock wave. Degree of ionization can be measured by dividing the concentration of former with that of latter.

Just after the laser strike, the temperature of plasma reaches to about 20,000 K. This hot plasma rapidly cools down and emit radiations of characteristic wavelengths. After few moments of the pulse strike, the plasma temperature is in the range of 5000-6000 K and electron density in the range of 10^{17} cm^{-3}.

3.3 Light Emitted from the Plume

Light emitted from the plasma is taken to a spectrometer through optical fibers. Optical fibers are tiny tubes which can carry light waves by continuously bending or reflecting it from its inner surface. It can be used to bend a light path with much ease. In the spectrometer, different special crystals are fitted which helps in resolution of incoming light into its constituent wavelengths. It works on the principle of dispersion of light through a diffraction grating. Obtained data is transferred to a computer via USB. Software installed in the computer, draws a well-defined graph of intensity verses wavelength instantly. The obtained graph is called a spectrum.

3.4 Spectrum

Analysis of the spectrum suggests that there are three types of spectrum:

- Continuous Spectrum
- Band Spectrum
- Line Spectrum

Continuous spectrum is of constant intensity with respect to wavelengths. Usually, blackbody spectrum is a type of continuous spectrum. It lies in infrared or visible region. For instance, continuous spectrum of x-rays obtained by decelerating electrons is a type of continuous spectrum.

Band spectrum is the series of closely spaced lines which combines to form a band. Spectrum obtained from molecules is a type of band spectrum. Molecular energy levels consists of close lying levels, transitions between them produces a band spectrum.

Atomic species give line spectrum. They are in the form of distinct peaks in the spectrum. It results from transitions between atomic levels of atoms or ions. Line spectrum is used in present work. When electron drops from higher level of energy E_2 to lower level of energy E_1, a photon is emitted of characteristic wavelength. Thus, obtained peaks have wavelengths associated with it but are a broadened around it due to other aspects.

3.5 Line Broadening

Quantum theory dictates that the energy of photon is exactly equal to the energy difference of the levels but actual spectral lines do have some broadening. It is due to different reasons discussed below:

Natural broadening is due to quantum limitation of Heisenberg uncertainty principle that any observer is unable to calculate some parameters with absolute certainty. Natural broadening is usually very negligible in calculations to produce a large error. Furthermore, it is inevitable to be present.

Atoms in a sample are in constant motion due to thermal energy. Moving atoms emits photon a shifted wavelength photon than supposed to be emitted by a stationary atom. This is called the Doppler Effect, which states that frequency of a wave gets shifted due to the motion of the observer. This is known as Doppler broadening.

Stark broadening is due to electric fields in plasma. It forces the peaks to have a Lorentzian profile, more pointed on the top and narrower width than Gaussian one. Stark broadening is used in present work to calculate electron plasma density.

4 Factors Affecting LIBS

Ablated plasma depends upon laser parameters, environment conditions and sample material. Some of important parameters of plasma include:

4.1 Ambient Condition

Beside the transition lines of the sample under consideration, transition lines of gases are also present in the spectrum. It is due to the breakdown of air in front of the sample, it may interrupt the quantitative analysis of the sample. It also has effect on the analytic performance of the sample. If the thermal conductivity of gases is more than that of plasma, plasma will rapidly cool resulting in lower temperature. On the other hand, more hot plasma is produced if thermal conductivity of ambient gases is relatively small. To overcome this problem, sample can be placed in vacuum and then irradiated by laser. But usually, it is not much necessary. [27, 28]

4.2 Laser Irradiance

The intensity and width of spectral lines increase with increase in intensity of laser beam. Energetic beam is sure to cause more electron temperature and electron density. Hence many spectral lines are observed with elevated intensities and widths. Increase in distance of the source from the target also diminishes the peaks. It is due to the fact that laser loses its energy while passing from the air. Musadiq at el [29] observed silver plasma by ND:YAG laser and

concluded that laser irradiance is directly proportional to spectral lines and inversely proportional to distance from the sample. Hanif et al [30] studies the characteristic of ZnO plasma using first harmonic and second harmonic of Nd: YAG laser. He observed that temperature of ablated plasma increase with laser irradiance and he also observed that width and intensity of spectral line increase with laser irradiance. However T_e and N_e attain saturation on a higher values of power density [31]

4.3 Spot size of the laser

If spot size of laser is small, it means there will be more density gradient. [32] Plasma will be localized and we can thus achieve higher temperatures. [33, 34] Convex lens is placed in the path of the laser to focus it on one single point. Lens converge the beam giving it the shape of the cone with its tip at the sample. Laser spot diameter can be calculated by:

$$\text{Spot diameter} = 1.27 \times f \times \boldsymbol{\lambda} \times \frac{M^2}{D} \tag{1.10}$$

D is diameter of beam before it is focused, f is focal length of lens and M^2 depends upon propagation of beam, calculated as under:

$$M^2 = \frac{D l \tau \, d_o}{4 f \lambda} \tag{1.11}$$

Above relation shows: $M^2 \alpha \frac{D}{f}$

It means that larger diameter beams can be focused to a single point by using lens of small focal length.

4.4 Sample Surface and Nature

Plasma parameters are also dependent upon nature of target. Several shots on the same point on the sample make crater which affects laser ablation. Stiffness of target is also a crucial factor. [35, 36]

4.5 Laser Wavelength

Ablation also depends upon laser wavelength. Laser of shorter wavelength, due to its penetration power is good for plasma creation than longer ones. [8] Thus temperature and electron density varies with the use of different harmonics. Nd:YAG laser is actually 1064nm wavelength but it is usually frequency doubled for irradiance. Since laser has different modes, there will be slightly different energy for each shot. [39, 40]

5 Pre-requisites for Quantitative Analysis

5.1 Optically Thin Spectral Lines

This is an important prerequisite for be sure to proceed with analysis. If the size of produced plasma is large, the emitted photons, due to de-excitation or recombination processes, are reabsorbed by the matter. This leads to inaccurate measurements of concentrations in the sample. It is due to the fact that the mean free path of radiation is less than plasma dimensions. This causes the peaks to become flattened at the top and diminish in intensity. Laboratory plasmas are usually optically thin because plasma dimensions are relatively small and much of the radiation emitted is not reabsorbed. Below mentioned equation is used to check whether plasma is optically thin or not:

$$\frac{I_1}{I_2} = \frac{\lambda_2}{\lambda_1}\frac{A_1}{A_2}\frac{g_1}{g_2}\exp\left[\frac{E_2 - E_1}{k_\beta T}\right] \tag{1.3}$$

This equation relates the intensity ratio calculated experimentally to theoretical values. In order to minimize the dependence on temperature, ratio of those lines are taken which have same upper levels or very close to each other.

5.2 Local Thermodynamic Equilibrium (LTE)

Local thermodynamic equilibrium is necessary to have a well-defined temperature for the system. If energy lost by radiation is smaller than that involved in the other processes involving material species or if the time between two collisions is small as compared to the time of subsequent change then plasma is said to be in local thermodynamic equilibrium

Saha–Boltzmann equation and Maxwell distributions are valid only for LTE plasma. If ablated plasma has a following characteristics than it is in LTE:

- Energy levels follow Boltzmann law distribution.
- Ionization, excitation and dissociation occur at a same temperature.
- Intensities of lines emitted should be according to Planck Equation.

Local thermodynamic equilibrium condition is satisfied after 1-2 ms of laser strike. Maxwell Distribution Criterion and McWhirter criterion [20, 21] are usually used to check the LTE condition of plasma. Maxwell Distribution Criterion requires the below mentioned equation to fulfil:

$$\mathrm{Ne} \geq 1.6 \times 10^{12} T^{\frac{1}{2}} (\Delta E)^3 \tag{1.4}$$

Here, T is temperature; ΔE is difference between energies of upper and lower levels whereas Ne is Electron number density.

6 Quantitative Analysis

Quantitative analysis involves the estimation of weight percentages of elements present between them. Such an analysis is essential in many fields of life especially in pharmacy. Two methods are usually used:

- Calibration Curve (CC) Method
- Calibration Fee (CF) Method

6.1 Calibration Curve Method

Calibration Curve method is a method to get good estimate of concentration. It involves the drawing of a calibration curve from the data for different samples of a single spectral line. Intensity of the spectral line of a specie is related to number density via:

$$I_{ki} = A_{ki} n_k^s \frac{hc}{\lambda_{ki}} \tag{1.5}$$

I_{ki} is intensity of emitted line, A_{ki} is transition probability between two levels, h is Planck's constant, c is speed of light, n_k is number density of upper level. Thus, intensity of line emitted is proportional to number density of the upper level [45-50]. The plot is a straight line with positive slope confirming a direct relationship. To order to calculate the concentration of specie, intensity of that spectral line is checked in the graph. The corresponding concentration on the x-axis is the required result. Artificial Neural Network (ANN) and Partial Least Square (PLS) are the methods in use if cc method fails. [51, 52] The major drawback of this method is that it requires a sample with a known composition similar to unknown sample which is not possible in each case.

6.1.1 Limit of Detection (LoD)

Limit of detection is the minimum concentration which can be accurately measured using specified calibration curve technique. It is calculated from the slope of calibration curve and the standard deviation of noise. It shows the signal to noise ratio. The formula set for limit of detection measurements is: [23]

$$LoD = \frac{3\sigma}{b} \tag{1.6}$$

Here, b is the slope of the calibration curve while σ is standard deviation of noise taken around the spectral peak.

6.2 Calibration Free LIBS Method

This CF is more widely used for quantitative analysis with LIBS because no reference sample is required in it. Electron density and temperature are determined from the data and

used in determination of percentage composition. It is compulsory that the plasma must be optically thin and in Local Thermal Equilibrium (LTE). Optically thin lines are carefully selected and LTE condition is satisfying by a condition on Ne. This condition is met 1-2 ms after plasma formation.

In CF-LIBS, electron temperature and electron number density are two most important parameters to be calculated. Electron temperature of plasma is measured in two different ways described below:

- Intensity Ratio Method
- Boltzmann Plot Method

6.2.1 Intensity Ratio Method

In intensity ratio method, ratio of two lines of same species is taken, temperature can be calculated by comparing it with other factors. [22] We use the equation (1.3) to get the electron temperature. If energy of upper levels and other parameters of both lines is known, one can get the temperature by comparing the intensities of different lines. Furthermore, by taking measurements of different lines, error can be reduced by averaging the temperature thus obtained.

6.2.2 Boltzmann Plot Method

While, Boltzmann plot is a graph with energy of upper level on the x-axis and $\lambda I/gA$ on the y-axis. We have to draw Boltzmann plot for each species. Plot should be straight line with decreasing slope. Measurements of slope give the temperature while measurement of intercept gives the concentration of element whose Boltzmann plot is plotted. Boltzmann plot method is usually employed to get plasma temperature. Only the lines which are optically thin and free from self-absorption effects are chosen to draw Boltzmann plot to get accurate measurement of temperature.

6.2.3 Calculation of Electron Number Density (Ne)

Like temperature, electron number density is an important parameter used to estimate the concentration of each specie. [18, 19] LTE condition can also be checked by measuring electron number density. This is calculated by Lorentzian Fitting a peak and calculating the FWHM ($\Delta\lambda_{1/2}$). Equation used is: [24]

$$\Delta\lambda_{1/2} = 2\omega\left(\frac{N_e}{10^{16}}\right) + 3.5A\left(\frac{N_e}{10^{16}}\right)^{\frac{1}{4}}\left(1 - \frac{3}{4}N_D^{-\frac{1}{3}}\right) \times \omega\left(\frac{N_e}{10^{16}}\right) \qquad (1.7)$$

Stark Broadening parameter ω should also be in hand to use above equation. First term is electronic contribution in broadening while second term is the ionic contribution.

Ionic contribution is usually small and thus ignored. Here, ND is number of particles present in Debye Sphere which is calculated by the formulas: [25, 64-66]

$$N_D = 1.72 \times 10^9 \frac{T^{3/2}(eV)}{N_e^{1/2}} \quad (1.8)$$

Hα line is usually best to calculate electron number density by using the relation: [26]

$$\Delta\lambda_{1/2} = 0.549 \times \left(\frac{N_e\,(cm^{-3})}{10^{17}}\right)^{0.67965} \quad (1.9)$$

7 Applications, Merits and Demerits of LIBS

7.1 Applications of LIBS

LIBS is used in many fields for elemental analysis of samples including [11-17]

- It is used for analysis of stainless steel which has many elements
- It is used as a detective tool for explosive materials and chemical weapons
- It is used to explore the space
- It is used to different biological samples of plants etc.
- It is used to ensure that the food is safe
- It is used in as a track in nuclear reactors
- Nowadays, femtosecond lasers are used in the field of nano science

7.2 Merits of LIBS

- It is fast and requires no sample preparation which could results in sample contamination.
- Samples having any state of matter can be used
- It require a very small amount of sample.(about 1mm)
- It requires the destruction of very small amount of sample
- Procedure is very simple to follow
- It can be used with Raman and LTF to analyze molecules
- With many pulses of light one after the other, in depth profile of the sample can be achieved.

7.3 Demerits of LIBS

- Accuracy and precision are not yet up to the mark.
- Due to selection of very small portion, in-homogeneity may cause the calculated concentration to deviate from the original.
- They are costly and they are still a complex system
- Self-absorption and spatial overlap also causes us to reach at wrong results.

8 Techniques Used for Comparison

8.1 Energy Dispersive X-ray Spectroscopy (EDX)

In this type of technique, an excitation source, usually energetic electrons, are used to excite the core electrons creating a vacancy. Outer electrons de excite to lower level to fill that vacancy. These de-exciting electrons emit characteristic x-rays. A solid state detector is used to measure the energy of emitted photons. As the energy of emitted photon is related to the difference between the upper and lower level, detection and quantification becomes possible. This is normally used with electron microscope, where electrons are used to study the morphology of a sample.

There are two important parts of EDX setup. First is excitation and second is X-ray detector. Excitation source is usually electron microscopes (SEM or STEM), where electrons are emitted via thermionic emission and further accelerated with step voltages. These speedy electrons are then focused on the sample by magnetic lenses which are actually anodes with a hole through. Detector is usually a crystal of Si (Li) detector cooled by liquid nitrogen. Nowadays, Silicon Drift Detectors (SSD) are also used which are cooled by Peltier cooling systems. EDX is usually an extension in Scanning Electron Microscopes.

8.2 X-ray Fluorescence Spectroscopy

X ray Fluorescence Spectroscopy (XRF) is a wavelength dispersive spectroscopic technique, in which x rays are shined on the sample under observation. The impinging photons excite or ionize the core electrons due to their large energies. Outer electrons jump down to fill the vacancies thus created and emit photons of characteristic wavelength in x ray region.

For the detection purposes, different detectors are installed to detect different region of wavelengths. Every detector has its own mono chromator crystal, detector and electronics. Output radiations are first diffracted by a crystal and resolution of wavelengths is thus obtained.

XRF is considered perhaps the most accurate method to detect and quantify a sample. Owing to its WDS nature, it is more reliable however lighter elements are difficult to measure because of the low energy and penetration power of their characteristic x rays. It is widely used in atomic analysis of metals, ceramics and glasses. Forensic science and palaeontology greatly depend upon it.

9 Aim of the present work

Aim of this work is to compare the results of compositional analysis by LIBS with Energy dispersive X-ray spectroscopy (EDS) and x-ray fluorescence spectroscopy (XRF). LIBS still not a standard technique and many research papers have been published on compositional analysis by LIBS. On the other hand, EDS and XRF are considered as most accurate techniques for quantification of the samples especially metallic ones. XRF is more accurate and reliable due to its wavelength dispersive nature.

Zn and Al both are metals with atomic numbers 30 and 13 respectively. Al is a lighter element as compared to Zn. Mixture of these two elements makes alloys having many uses. ZA (Zinc Aluminium) alloys are used in the place of bronze, cast iron etc. They are easy to melt and high cast strength alloys having good bearing properties. There are three famous alloys (ZA8, ZA12 and ZA27) which are widely used named on the basis of concentration of Aluminium present in it, (ZA8 is 8% Aluminium). These are important alloys used in galvanizing and die casting.

Chapter No. 2

Experimental Setup

Experimental setup consist of second harmonic Q-switched Nd:YAG laser, a Avantes spectrometer and data acquisition system. Laser pulse has energy of in hundreds of mJ with pulse duration of 5 ns and repetition rate of 10 Hz [53-57]. "Avasoft 8" is the software used to set the parameters of the laser light. Furthermore, nova-quantel is used to measure the pulse energy. A convex lens is used to focus the beam to a single spot on the sample, mounted upon a rotating stage. Purpose of rotation is to insure that each pulse of laser gets fresh space of the sample. Its benefits are twofold. Firstly, non-uniformity of sample does not disturb the result. Secondly, incorrect measurement of the plasma parameters due to crater in the sample produced by any previous shot can be avoided.

Optical fibre is used to collect light emitted due to plasma ablation. It guides the light to four spectrometers, each covering the range of about 200 nm. Total range of these spectrometers is from 250 nm to 900 nm. The spectrum is recorded and can be viewed on the computer and at the same time AvaSpec detection system.

The different components of instruments used are listed below

- AvaSpec (HS1024×58)/122TEC) spectrometer
- Nd:YAG laser
- Convex lens
- Fibre optics
- A Computer
- AvaSoft 8 software

1 Laser Source

In this experiment, laser is perhaps the most important part of the apparatus. It produces breakdown of the sample. In Chapter 1, brief history and working principle of laser is mentioned. In order to get better understanding of laser, its working with different systems are briefly discussed. Furthermore, its uses and types are mentioned.

1.1 Working

The lasing material commonly known as active medium is placed between two mirrors. One of which is partially reflecting and other totally reflects the incoming light. It is then pumped to higher level from the ground level with either flash lamp or electric discharge. With pumping in action, the population of excited state continues to increase. After considerable pumping, population inversion state is achieved. Now a photon from spontaneous emission

causes the atoms to decay via stimulated emission. With constant circulation between mirrors, the effective length of active media is increased many times and light is amplified. This light passes out by the partial reflecting mirror. Laser can be used to work in pulsed mode with high power output typically in megawatts by the introduction of shutter in the cavity.

The photons moving along the axis are lost as an output or are lost by scattering, absorption and diffraction at the mirrors. To reduce the diffraction effects, mirrors are usually spherical in shape.

1.2 Multilevel Laser System

Laser operates between two energy levels of atom, but other close lying levels also play important role in making laser possible. Different systems to produce laser were proposed and are in use.

1.2.1 Two level Laser System

In two level system, atom has two energy levels for the photons to oscillate. They are optically or electrically pumped from the ground level E_1 to excited level E_2 as shown in fig 1. Upon de-excitation, one photon is emitted of energy equal to the difference of energies of upper and lower level i.e. E_2- E_1. Suppose at an instant of time, the upper level population (atoms present in the upper level) is N_2 while lower level has N_1 atoms, then the condition of population inversion is achieved when $N_2 > N_1$.

We can easily prove that in such a situation it is impossible to have population inversion. At most one can get to $N_2 = N_1$. Actually there is no metastable state in such a scheme. We have to move to two or three level laser scheme in order to produce laser.

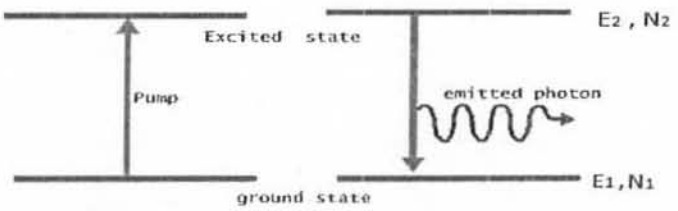

Fig 1 *Energy level diagram of two level laser system*

1.2.2 Three Level Laser System

In three level laser system, three levels of the atoms of active medium are used in lasing. Suppose energy levels are E_1, E_2 and E_3 with cross ponding population density N_1, N_2 and N_3 respectively as shown in fig 1.2. E_1 is the ground level while E_3 is upper level. Laser works between E_1 and E_2.

Under normal condition, upper states are not occupied and all atoms lie in their ground state, i.e.

$$N_1 \approx N \quad \text{and} \quad N_2 \approx N_3 \approx 0$$

Atoms are pumped from ground state E_1 to upper state E_3 optically or electrically. If pumping continues to operate for long, most of the atoms are excited to higher levels. Atoms decays from E_3 to E_2 almost instantly. But the next decay is not equally probable. Thus, atoms continue to pile up in state E_2. In this way, population of excited state becomes more than that of ground state, i.e.

$$N_2 - N_1 > 0$$

Population inversion is achieved and laser starts. But in three level laser system, it is necessary to pump the half of population to excited level to achieve population inversion. For this purpose active medium must be strongly pumped.

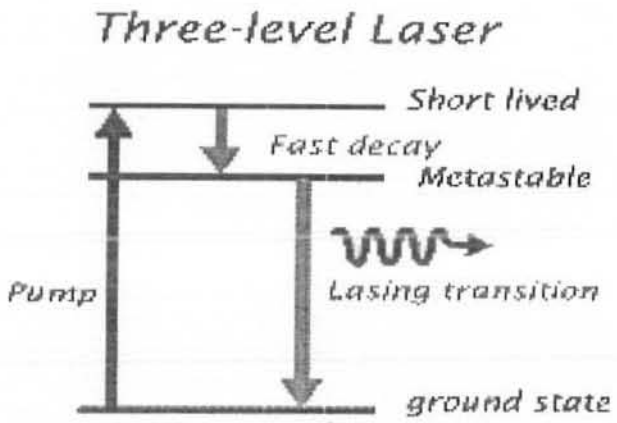

Fig 2 *Three level laser diagram*

1.2.3 Four Level Laser System

In four level laser system an active media have a four energy level E_1, E_2, E_3 and E_4 with their cross ponding population densities are N_1, N_2, N_3 and N_4 respectively. Atoms are excited from ground level E_1 to excited level E_4 then from E_4 atoms are spontaneously decayed towards E_3 state. E_3 is called metastable state. Life time of E_3 is more as compared to excited state so laser action is achieved in between E_3 and E_4. Only few atoms are excited towards the upper level in order to achieve the population inversion so four level laser system is more effective as compare to three level laser system. Pumping energy is higher than laser energy in both laser schemes.

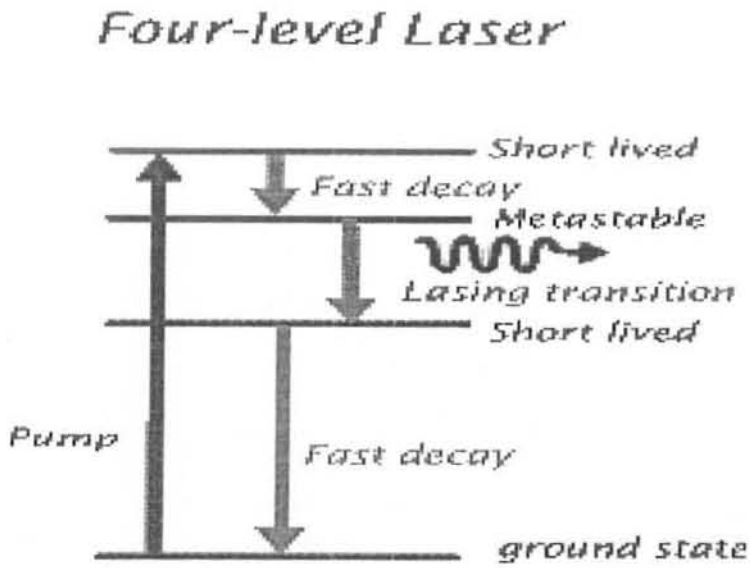

Fig 3 *Four level laser system*

1.3 Important Properties

1.3.1 Mono-Chromaticity

Mono-chromaticity means having single color. This is perhaps the very basic and the most important property of laser. Laser is more monochromatic than other light sources. This is because of the peculiar nature of stimulated emission which emits photons of same energy moving in same direction.

1.3.2 Coherence

Two beams of light having no phase difference or phase difference of even multiple of pi are called as coherent. There are two types of coherence, temporal and spatial one. Temporal coherence is the time duration for which waves remain coherent while spatial coherence is related to area on which waves are coherent. Laser beam is more coherent than any other light source. This is due to stimulated emission rather than spontaneous emission.

1.3.3 Directionality

Laser light is very directional. It can be made to focus on a small target in contrast to other light sources which diverge in all directions. This peculiar property is very crucial for so many uses of laser light.

1.3.4 Brightness

Brightness means power emitted per unit solid angle per unit area. Due to the continuous motion of photons in the cavity, the number of photons is very large thus, laser light is very

bright than other light sources. It is therefore used in cutting of materials. For example brightness of ND:YAG laser is in the orders of $10^{21}Wm^{-2}Sr^{-1}$ which is several order of magnitude more than that of our sun.

1.4 Types of Lasers

Different materials can be used as active medium for laser. Below are the types of laser systems w.r.t their active media:

1.4.1 Solid State Lasers

In solid state lasers, the active medium is a crystal doped with transition metals or rare earth materials. Different wavelengths are achieved by doping of different materials. Optical pumping is best option to achieve population inversion. Ruby and Nd:YAG lasers are important solid state lasers.

1.4.2 Gas Lasers

The active medium of gas lasers is mixture of gases which is pumped by collisions of electrons in a gas discharge tube. Wavelength of such lasers ranges from ultraviolet to infrared. Example of gas lasers are helium-neon laser, nitrogen lasers and carbon dioxide lasers.

1.4.3 Dye Lasers

Dye lasers are usually optically pumped with the help of flash lamps or other lasers. Examples include Rhoda mine 6G.

1.5 Applications of Lasers

From the advent of laser, scientists starting using laser in many areas. Nowadays, it is used in many areas of life due to these peculiar properties. [1, 2, 6] Some of them include:

- Medical uses
- Warfare
- Cutting and welding in industries
- Separation of isotopes
- Telecommunication
- Security means
- Spectroscopy and other laboratory equipment
- Computer drives

1.6 Nd:YAG Laser

Laser used in the experiment is a Nd:YAG laser. It is a solid state laser which is pumped by flash lamps. It can be used in continuous mode as well as pulsed mode. In this experiment pulsed laser is used as it produces more energetic laser. Neodymium (Nd^{+3}) acts as an active

medium. It is a four level laser scheme. Atoms are pumped from $^4I_{9/2}$ to $^4F_{5/2}$ by flash lamps. They carry out a fast de excitation to $^4F_{3/2}$. $^4F_{3/2}$ is a meta-stable state and transition to ground state is only possible by stimulated emission. Now atoms carry out a lasing transition to lower state $^4I_{11/2}$ with the help of another photon. Atoms again drop out instantaneously to ground state. It is a 1% efficient laser giving of light with wavelength of 1064nm which can be shifted to its second harmonic.

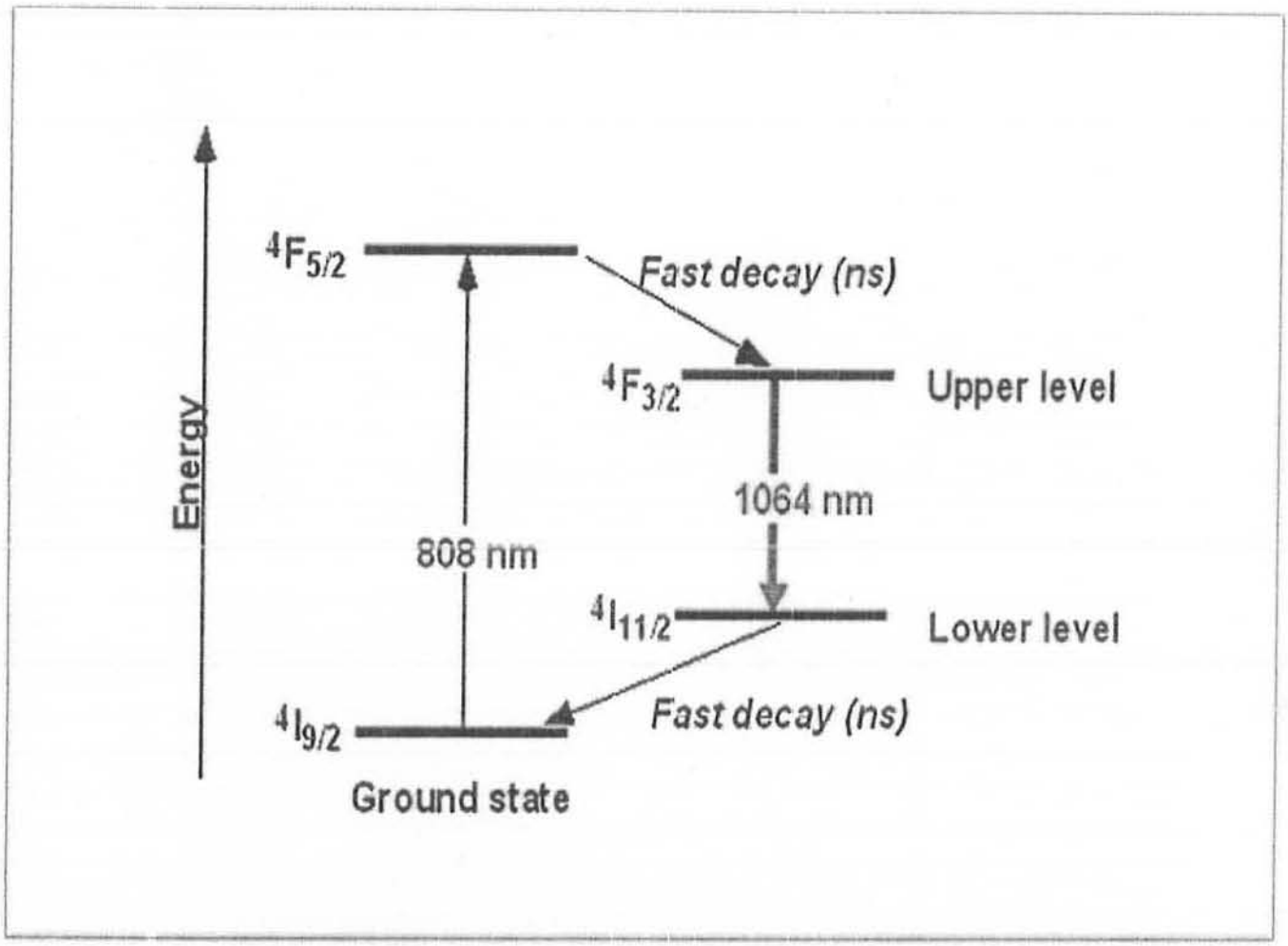

Fig 4 *Energy level diagram of Nd: YAG laser*

2 AvaSpec (HS1024×58)/122TEC) spectrometer

The function of a spectrometer is to detect the wavelengths of light emitted from the cooling plasma and plot a graph w.r.t intensity on the computer. It works on the principle of dispersion of light when passed through a diffraction grating. Four high resolution spectrometers (as low as 1.2 nm) are installed covering a range of 200-1160 nm. Details of the spectrometers is tabulated in Table 1. The diffracted light from the spectrometer is detected by

ULS 3648 detector. Three thousand six hundred and forty eight detectors are present in the spectrometer which give high resolution to our system. This whole mechanism is connected to the computer via a USB port. USB is fast port with 480Mbit/sec speed. With all this electronics, it only takes 5.24 ms to make a complete scan.

AvaSoft 8 software installed on the computer helps in control and display of the spectrum. It controls the integration time, averaging and smoothing number. Since the detector can produce small dark currents even not exposed to light, a rigid smoothing parameter is necessary to ensure that no information is lost. AvaSoft 8 sets a smoothing parameter as well. The main components of the spectrometer are labelled in Fig. 5.

Table 1: *The properties of spectrometers used*

Spectrometer Serial No	Range (nm)	Grating Parameter (lines/mm)	Slit Size (μm)
1	248-420	1800	10
2	416-562	1800	10
3	557-678	1800	10
4	666-882	1200	10

3 Optical Fibre

Optical fibre is a device which allows the light from the plasma to reach the spectrometer. It is made of quartz crystal and plastic. It is made up of several fibres which allow light to pass despite the fibre is curved. It is important component without which system is subject to many limitations.

The working principle of optical fibre is the total internal reflection of light while passing through the fibre or light can be continuously bent with the use of materials having varying refractive index. Refractive index goes on changing as one moves from the axis of the fibre to the edge. In this way light can be made to travel long distances despite the presence of curvature. It is used to send electronic signals to intercontinental distances.

Parameters of the fibre used by us are:

- Fibre type: HIGH-OH
- Clad/ Core ratio: 1:1.1
- Fibre core diameter: 600μm
- Epoxy used: Epotek 353

- Connector type: SMA-905
- Length: 22 inches
- Numerical aperture: 0.22
- Fibre buffer material: Polyimide

Chapter No. 3

Quantitative Analysis

Different techniques used for compositional analysis and two techniques are used. First is calibration curve method and second is calibration free CF LIBS. In our experiment, one line calibration free LIBS is carried out for quantitative analysis and the results are compared.

Ciucci [58] initially developed a calibration method in which composition is acquired from intercepts of a Boltzmann plot and by using slope of plot temperature is to be determined. Method developed by Ciucci had been used in different research papers as an quantitative analysis [8] of different type of materials but this method have a major drawback that is if one wants to calculate the total concentration or composition of targeted sample then a Boltzmann plot of each specie is necessary but it is not possible in each case because at least 3 to 4 spectral lines are required to draw a Boltzmann plot and it is not necessarily true that each species have a sufficient number of spectral lines.

To surmount a problem faced by a Ciucci another CF-LIBS technique developed by Goma et al [62, 63] that based on algorithm in which theoretically and experimental acquired values are matched. Theoretical values determined from ratio of number density of neutral species to ratio of density of ionized species and experimental value based on optically thin spectral lines. The fundamental requirement is that spectral lines that are used for quantitative analysis should be optically thin and in LTE.

Before proceeding with analysis, spectral lines are carefully selected in order to get minimum self-absorption. This is done by selecting spectral lines which follow some conditions:

- Resonance lines or the lines having lower energy less than 6000 cm^{-1} are usually ignored.
- Lines having transition probability less than $2x10^6$ are ignored as it is time attributable to plasma variations.

1 Compositional analysis by Calibration Curve Method

In this technique, calibration curve are drawn for known samples, which differs in concentration of species. A graph is plotted between concentration and intensity of spectral lines called calibration curve. Such curve should be straight line. Now, spectral line intensity is checked in this graph for unknown concentration. In this way concentration of unknown

sample can be easily measured. This method is subject to limitations as it is impossible to have a known sample most of the times.

1.2 Limit of Detection (LoD)

Limit of detection is an important quantity which can be measured with calibration curves. It reflects the precision of the instrument. It is an important check of the instrument to be used for any purpose. Limit of detection is calculated by the relation (1.6)

2 Quantitative Analysis using CF-LIBS

Usually it is not possible to have reference samples, so that a calibration curve can be drawn. To overcome this problem, a calibration free LIBS technique is devised. Calibration free LIBS technique is used in different papers to get the quantity of each element of the sample.

In this method Boltzmann plots are plotted to get temperature and electron density of each species. These plasma parameters are then used in quantitative analysis of the sample.

2.1 Boltzmann Plot

The population density of excited state is written below: [85]

$$n_k^s = n^s \frac{g_k}{P(T)} \exp\left[-\frac{E_k}{k_\beta T}\right] \tag{3.1}$$

Here, s denotes the specie and k is used to denote the upper level, n is population density and g is the statistical weight.

Whereas partition function P (T) can be calculated as:

$$P(T) = \sum_k g_k \exp[-\frac{E_k}{k_\beta T}] \tag{3.2}$$

Now, the intensity of emission line is:

$$\mathrm{I_{ki}} = \mathrm{A_{ki} n_k^s} \frac{\mathrm{hc}}{\lambda_{\mathrm{ki}}} \tag{3.3}$$

Where h is plank constant and c is speed of light. Re arranging:

$$\frac{\mathrm{I_{ki}}\lambda_{\mathrm{ki}}}{\mathrm{A_{ki}hc}} = \mathrm{n_k^s} \tag{3.4}$$

Compared with above equation (3.1) becomes:

$$I_{ki} = A_{ki} n^s \frac{hc}{\lambda_{ki}} \frac{g_k}{P(T)} \exp\left[-\frac{E_k}{k_\beta T}\right] \tag{3.5}$$

This measured intensity is also affected by the efficiency of collection system, thus above equation can be better expressed as:

$$\overline{I_{ki}} = F C^s A_{ki} \frac{hc}{\lambda_{ki}} \frac{g_k}{P(T)} \exp\left[-\frac{E_k}{k_\beta T}\right] \tag{3.6}$$

Where, $\overline{I_{ki}}$represent integral line intensity, Cs is the concentration and F is an experimental factor which takes into account the consideration of efficiency of the collection system. By taking the logarithm of above equation:

$$\ln\left[\frac{\lambda_{ki}\overline{I_{ki}}}{hcA_{ki}g_k}\right] = -\frac{E_k}{k_\beta T} + \ln\left[\frac{FC^s}{P(T)}\right] \tag{3.7}$$

Compare Eq. with a linear form$y = mx + q_s$

Then,

$$y = \ln\left[\frac{\lambda_{ki}\overline{I_{ki}}}{hcA_{ki}g_k}\right]; x = E_k ; m = -\frac{1}{k_\beta T}; q_s = \ln\left[\frac{FC^s}{P(T)}\right] \tag{3.8}$$

Each point on a Boltzmann plot represents a spectral line. While plotting the Boltzmann plot energy of upper level taken along the X-axis and $\ln\left[\frac{\lambda_{ki}\overline{I_{ki}}}{hcA_{ki}g_k}\right]$ taken along the y-axis

As $m = -\frac{1}{k_\beta T}$ or:

$$T = -\frac{1}{k_\beta m} \tag{3.9}$$

Reciprocal of slope of plot gives temperature of ablated plasma and concentration or mass composition of any sample can be calculated by this relation or modified form 3rd part of equation (3.8):

$$FC^s = P(T)e^{q_s} \tag{3.10}$$

If plasma is optically thin and fulfil the LTE condition than slope of plot of each species will be same or close to each other but intercepts, as they account to concentrations, can be or should be different.

2.3 Determination of Electron Number Density (N_e)

Electron number density is required plasma parameter which is used in quantification. N_e is calculated by measuring Stark broadening. It can be calculated by any optically thin spectral line whose value of stark broadening parameter is known. Formula used is: [71-73]

$$Ne = \left(\frac{\Delta\lambda_{1/2}}{2w}\right)\times 10^{16}\,cm^{-3} \tag{3.14}$$

Here, $\Delta\lambda_{1/2}$ is the full width at half maximum. In this study, following Stark broadening parameters are used from literature. [67, 68]

Table 1: *Stark Broadening Parameters*

Spectral Line Wavelength (nm)	Stark Broadening Parameter (nm)
308.2	0.0045
309.27	0.0049
394.4	0.0037
396.15	0.0038

2.4 One line calibration Free Method

We can calculate the composition of an element using it only a single spectral line. Average is taken of the concentrations calculated from different lines. Using this method, population of neutral atoms are calculated using equation 3.11

$$n^{\alpha,z} = \frac{I\,P(I)}{A_k g_k} \exp\left[\frac{E_k}{KT}\right] \tag{3.11}$$

By using the temperature calculated by the Boltzmann plot, one can determine the concentration of neutral species. In order to get number density of ionized species, Saha-Boltzmann Equation was used: [69]

$$n_e \frac{n^{\alpha,z+1}}{n^{\alpha,z}} = \left(\frac{2\pi m_e k_\beta T}{h^2}\right)^{3/2} \frac{2P_{\alpha,z+1}}{P_{\alpha,z}} \exp\left[-\frac{\chi_{\alpha,z}}{k_\beta T}\right] \tag{3.12}$$

Where n_e represent electron density $n^{\alpha,z+1}$ is the density of atoms in singly ionized state, $n^{\alpha,z}$ is the density of atoms in neutral state $\chi^{\alpha,z}$ is the ionization energy, $P_{\alpha,z+1}$ and $P_{\alpha,z}$ are the partition functions of upper and lower charge state. Everything else has usual meanings. If the constants are put in the equation, it becomes: [62]

$$\frac{n^{\alpha,z+1}}{n^{\alpha,z}} = \frac{6.04\times10^{21}(k_\beta T)^{\frac{3}{2}}}{n_e} \frac{P_{\alpha,z+1}}{P_{\alpha,z}} \exp\left[-\frac{\chi_{\alpha,z}}{k_\beta T}\right] \tag{3.13}$$

If the concentration of neutral species is known, one can calculate the concentration of ionized ones by the use of above equation. This equation can also be used to calculate n_e if number density of both types of lines are already known. [74-77]

Equations 3.11 and 3.13 are multiplied together to get number density of ionized species. Then both these quantities are added together to obtain total number density. For example, for z=0 and α=Al, we have:

$$n^{\alpha} = n^{\alpha,0} + n^{\alpha,1}$$

Number densities are then converted to weight compositions by multiplication with atomic weights of each specie:

$$n^{\alpha*} = n^{\alpha} * A^{\alpha}$$

Whereas, A^{Al} is atomic weight of Al. Now, percentage composition is calculated by the relation:

$$C^{\alpha} = \frac{n^{\alpha*}}{\sum n^{\alpha*}} \times 100$$

Chapter No. 4

Results and Discussions

To study the comparison between LIBS and different other recognized techniques, five samples of varying concentration of Zn and Al were prepared. Zn was a resin here and Al is present small quantities (0.5, 1, 2, 5 and 10 Per Hundred Resin). Zn and Al were in fine powdered form (<10μm). Resin (Zn) is 3g for each pallet and Al is taken accordingly. Fine powdered mixture is pressed at high pressure for few seconds to form tough metallic pallets.

Each sample is first cleaned with methyl alcohol to remove dust and stains. It is then mounted in front of the focused laser source. The plasma on the surface of the alloys was generated by focusing the beam of a Nd:YAG laser at 532 nm, pulse energy 130 mJ and 2 μs delay between the laser pulse and the detection system. As soon as the plasma is generated, plasma plume expands perpendicular to the target surface and after a few micro seconds, it cools down and its emission spectrum contains characteristics spectral lines of the constituent elements. In Figs. 4.1 (a), (b) the emission spectra are presented covering the wavelength region from 200 to 700 nm. The major part of the 4.1 (a), (b) consists of the spectral lines of Zinc and Aluminum. The dominating lines belong to Zinc and Aluminum besides a couple of lines attached to the singly.

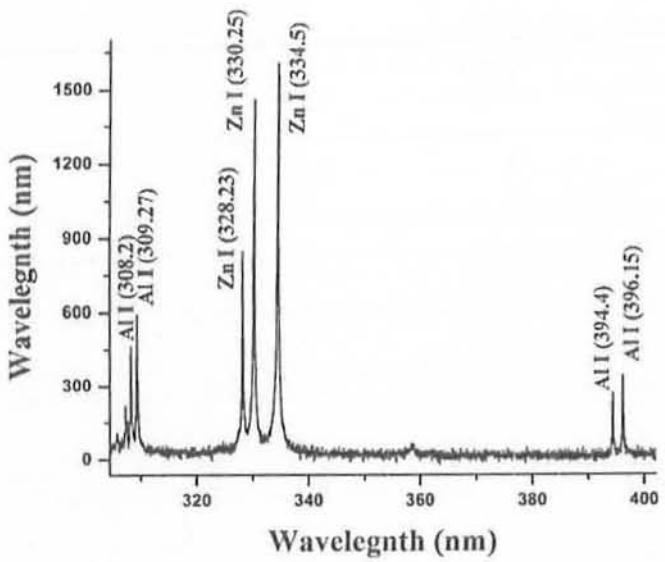

Fig 1 (a): *Optical emission spectrum of the Laser produced Zn-Al alloy plasma of the "sample D" covering the spectral region 300- 400 nm. The spectral lines of Al I and Zn I are assigned*

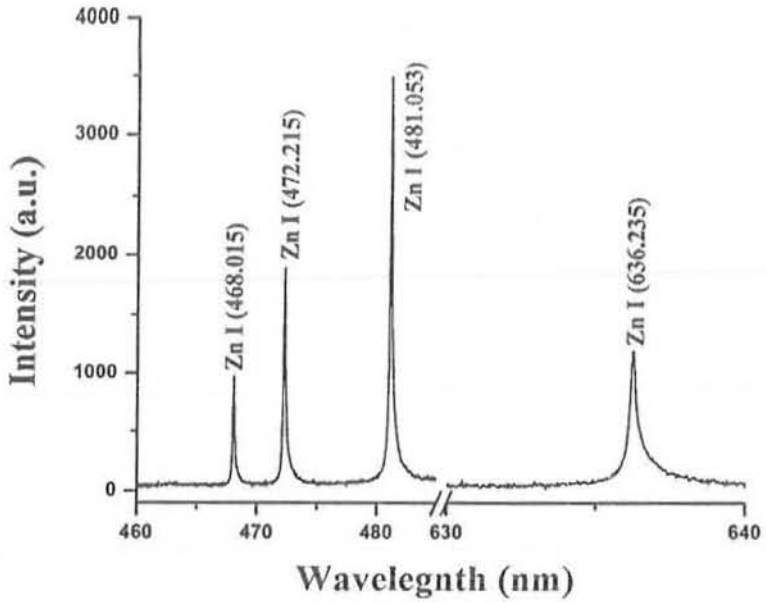

Fig 1 (b): *Optical emission spectrum of the Laser produced Zn-Al alloy plasma of the "sample D" covering the spectral region 460- 640 nm.*

Among the lines in the spectra, optically thin lines are checked by intensity ratio method discussed further in the chapter. Spectral lines situated on the spectra are 257.5, 308.2, 309.27, 394.4 and 396.15 nm of Al (I), while 328.23, 330.25, 334.5, 636.235, 468.015, 472.215 and 481.053 nm for Zn (I). There were no lines for Al (II) while some lines of Zn (II) were also present. The spectral data i.e. statistical weights and transition probabilities are mentioned in Table 4.1 are taken from NIST database. [86, 87]

Table 4.1: *Spectral lines used for quantification*

Wavelength (λ)	Statistical Weight (g_k)	Transition Probability (A_k) $\times 10^7$	Energy of Upper Level (E_k)
Al (I)			
257.5	6	3.60	38933.97
308.2	4	5.87	32435.45
309.27	6	7.29	32436.8
394.4	2	4.99	25347.76
396.15	2	9.85	25347.76

Zn (I)			
328.23	3	9.00	62768.75
330.25	3	6.70	62768.75
334.5	5	4.00	62772.01
636.235	5	4.65	62458.51
468.015	3	1.55	53672.24
472.215	3	4.58	53672.24
481.053	3	7.00	53672.24

1 Calibration Curve Method

Calibration curve for different spectral lines are drawn. Concentration is plotted along the x axis while intensities along the y axis. Straight line fit matching with the data points ensures an accurate calibration curve. Limits of detection were also calculated from these curves. Curves using different Al peaks along with background noise are shown in Fig 4.2 (a-d).

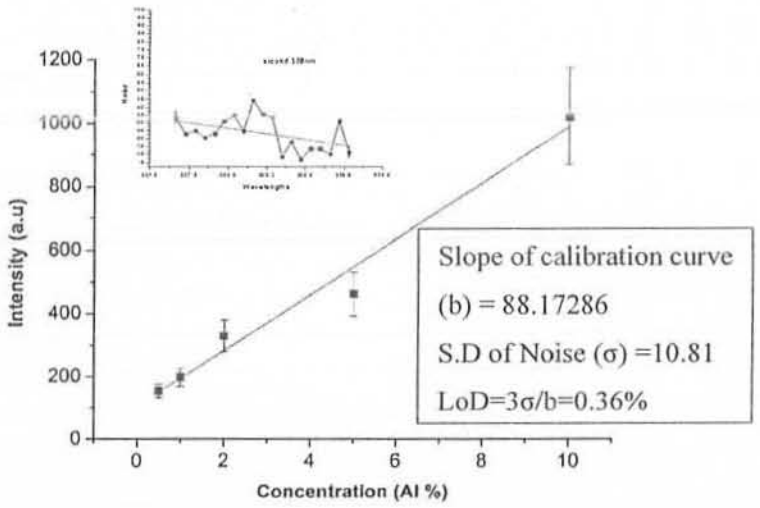

Fig 2 (a): *Calibration Curve of 308.2 nm line and deviation of noise signal*

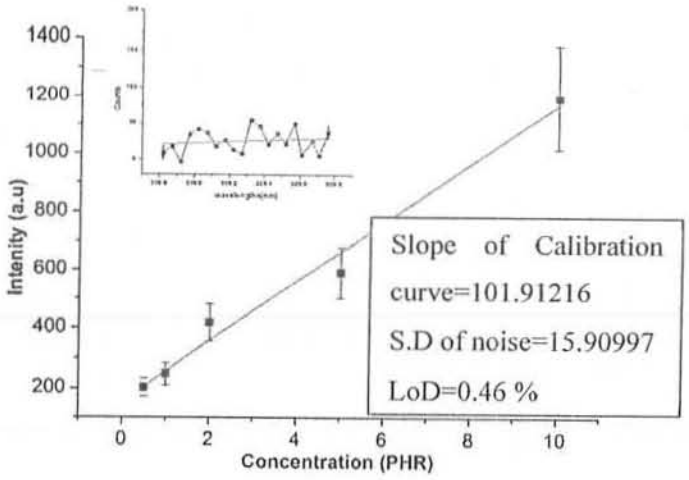

Fig 2 (b): *Calibration Curve of 309.2 nm line and deviation of noise signal*

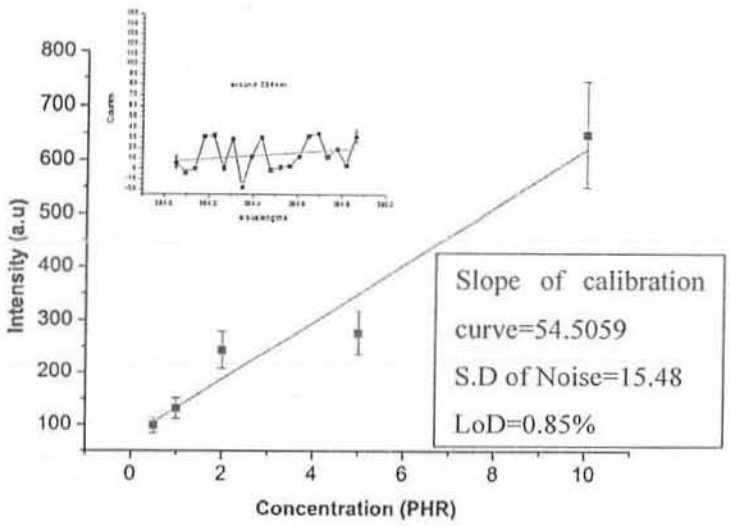

Fig 2 (c): *Calibration Curve of 394.4 nm line and deviation of noise signal*

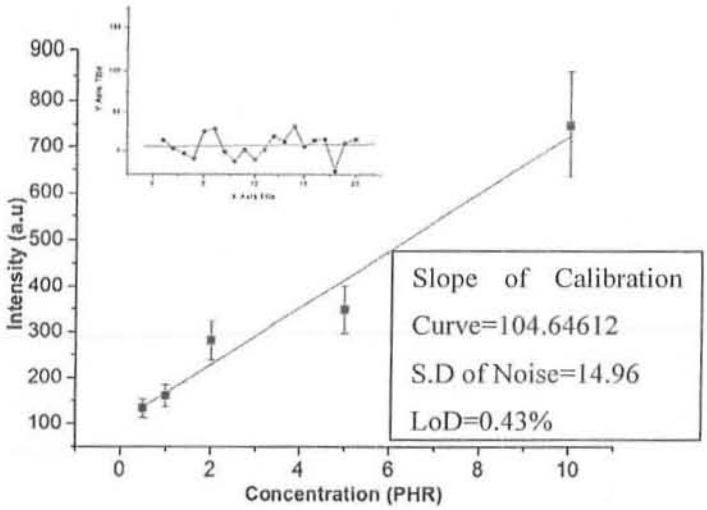

Fig 2 (d): *Calibration Curve of 396.15 nm line and deviation of noise signal*

Four peaks of Al (308.2, 309.2, 394.4, and 396.15) are used to draw these curves. Slopes of the curves range from about 50 to 100. Noise signal (shown in small) is taken around the required peak from the spectrum of pure resin. Standard Deviation of noise is between 10 and 15. Our calculated values range from 0.3 per cent to 0.8 per cent.

Compositional analysis with calibration curve is carried out by comparing the intensity of spectral line from the unknown sample on the curve. The respective percentage on the x-axis is the required concentration. If calibration curve of a series of samples is readily available, calibration curve is good technique to analyse samples.

2 Calibration Free Method

Calibration free method is carried without any reference sample. Due to this reason, it is widely used nowadays and researches have being carried out. In this method, spectral lines are carefully selected to draw Boltzmann plots. These plots are a requisite to get the value of electron temperature for the sample.

Electron numbers density is also required plasma parameter used in compositional analysis which are calculated by Stark Broadening.

2.1 Electron Temperature Measurement

Electron temperature is estimated by using Boltzmann plots of Al and Zn. Upper level is plotted along the x axis while ln ($\lambda I/gA$) along y axis. The slope of such a curve is used to estimate the temperature by the relation (3.9)

2.1.1 Boltzmann Plots using spectral lines of Al

Boltzmann plots for all samples are given below. Linearity of the curve is a check to be sure that our plasma is optically thin. Good linear behaviour of the Boltzmann plot serves as a check to be sure of the optically thin nature of the plasma. Furthermore, this condition is also checked by taking ratio of intensities and comparing it with theoretical values. Spectral lines used for analysis are 257.5, 308.2, 309.27, 394.4 and 396.15 nm

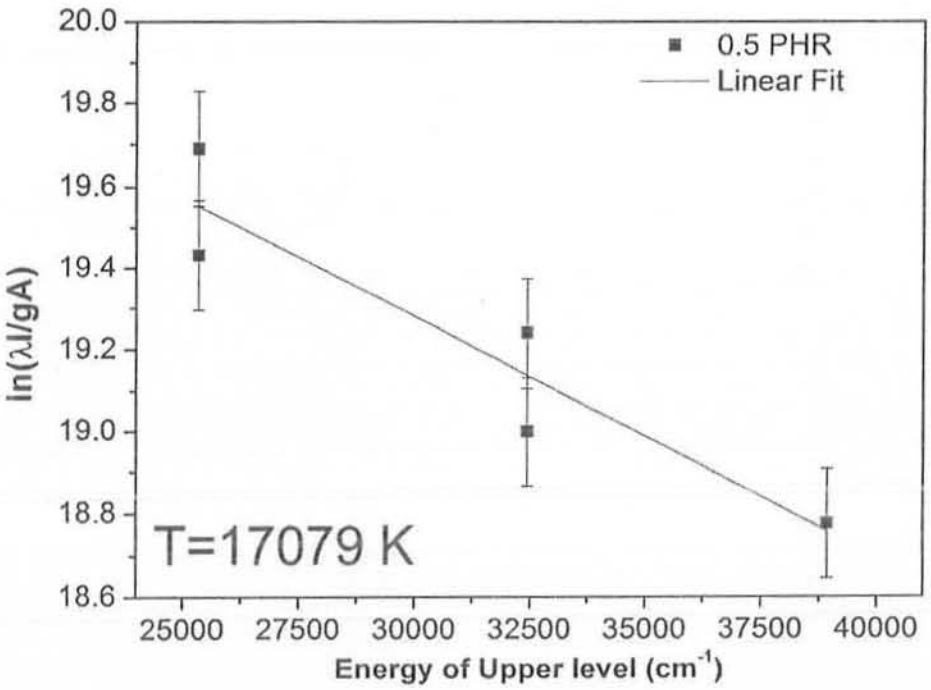

Fig 4 (a): *Typical Boltzmann-Plot. Emission lines of neutral Al from sample A are used for obtaining temperature.*

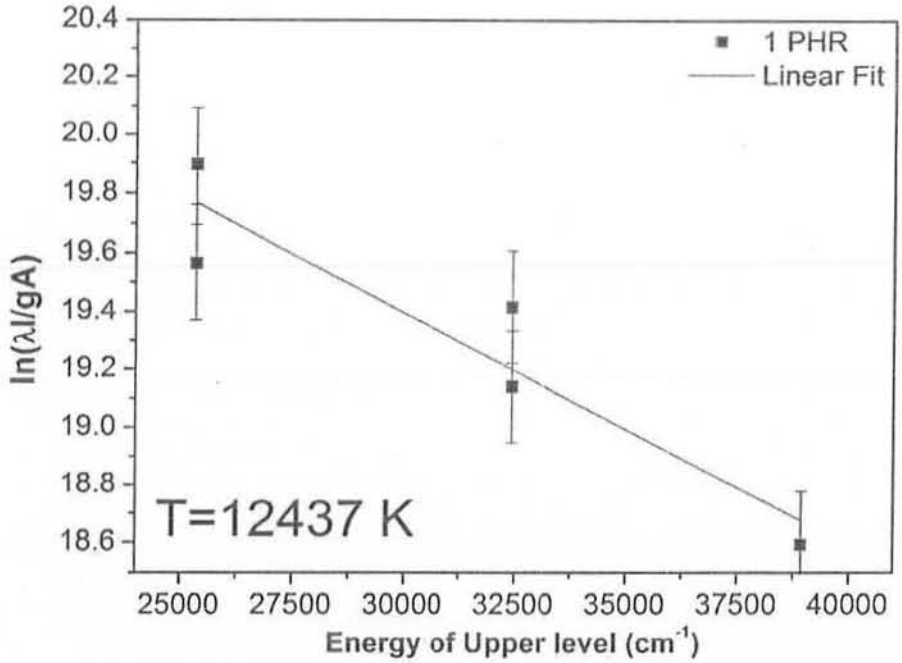

Fig 4 (b): *Typical Boltzmann-Plot. Emission lines from neutral Al of sample B are used for obtaining temperature.*

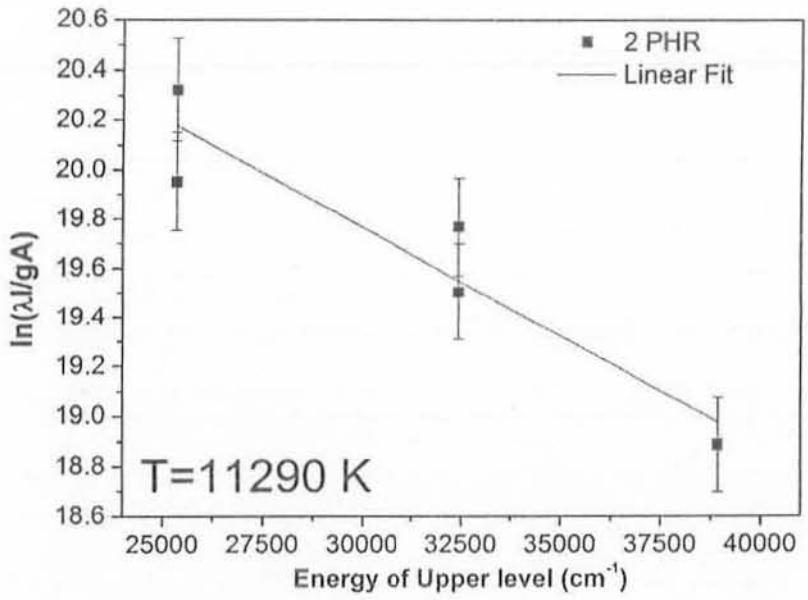

Fig 4 (c): *Typical Boltzmann-Plot. Emission lines from neutral Al of sample C are used for obtaining temperature.*

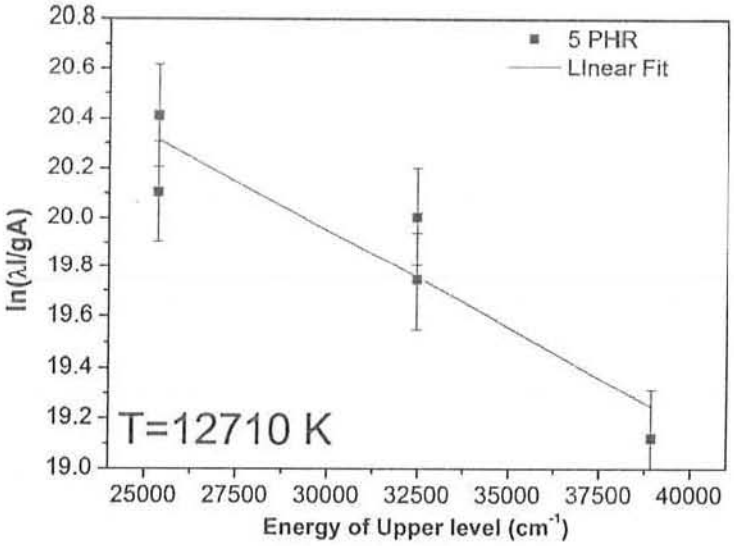

Fig 4 (d): *Typical Boltzmann-Plot. Emission lines of neutral Al from sample A are used for obtaining temperature.*

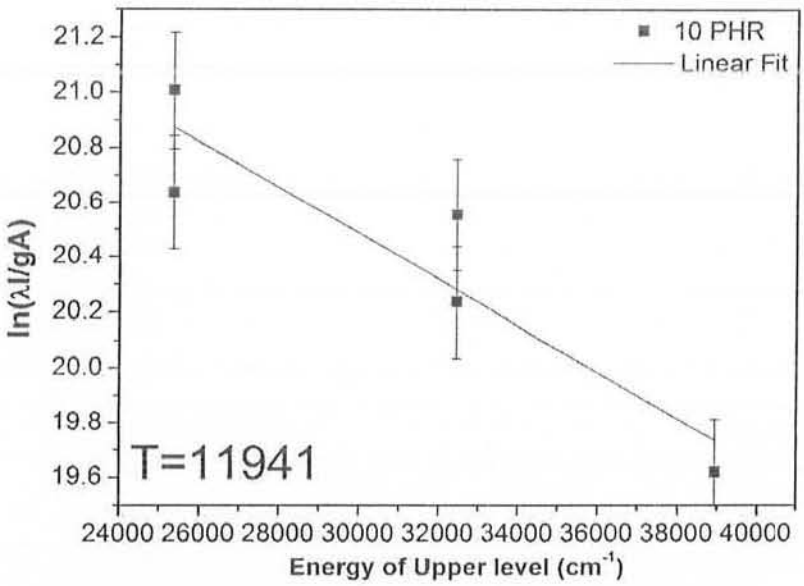

Fig 4 (e): *Typical Boltzmann-Plot. Emission lines from neutral Al of sample E are used for obtaining temperature.*

Excitation temperature for sample 0.5 PHR is about 17000 K whereas, other samples yield temperature round 12000 K. The elevated temperature of sample A shows that we are quite close to LoD of CF-LIBS method. The peaks corresponding to sample A are very diminished,

thus effects of noise becomes enhanced. All other temperatures are typical for laser ablated plasmas.

2.1.2 Boltzmann Plots using spectral lines of Zn

Boltzmann plots using spectral lines of Zn are given below. All samples have approximately same temperature in the range of 11000 K to 12000 K. Lines used to estimate temperature are 330.25, 334.5, 636.235, 468.015, 472.215 and 481.053 nm. The 328.23 nm line showed a deviating behaviour from the straight line and thus excluded.

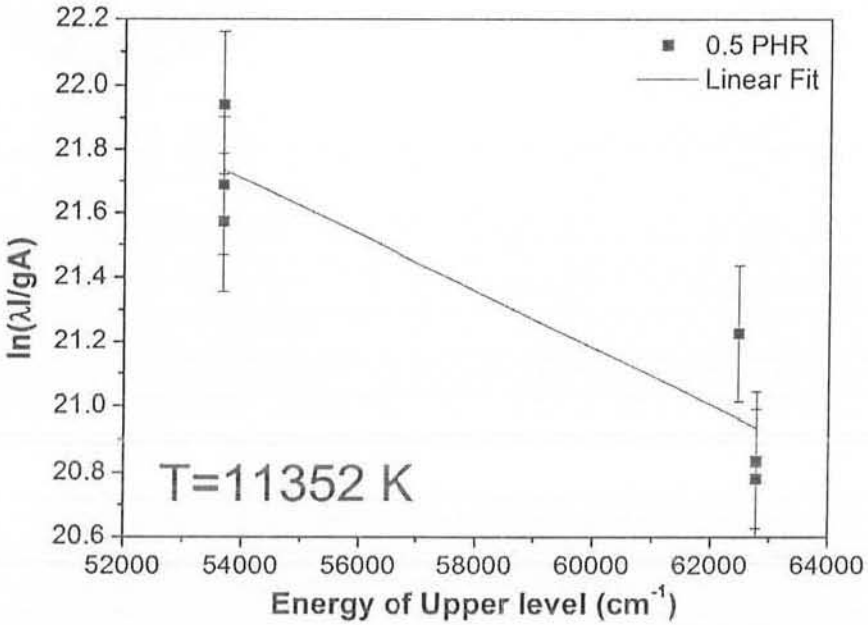

Fig 5 (a): *Typical Boltzmann-Plot. Emission lines of neutral Zn from sample A are used for obtaining temperature.*

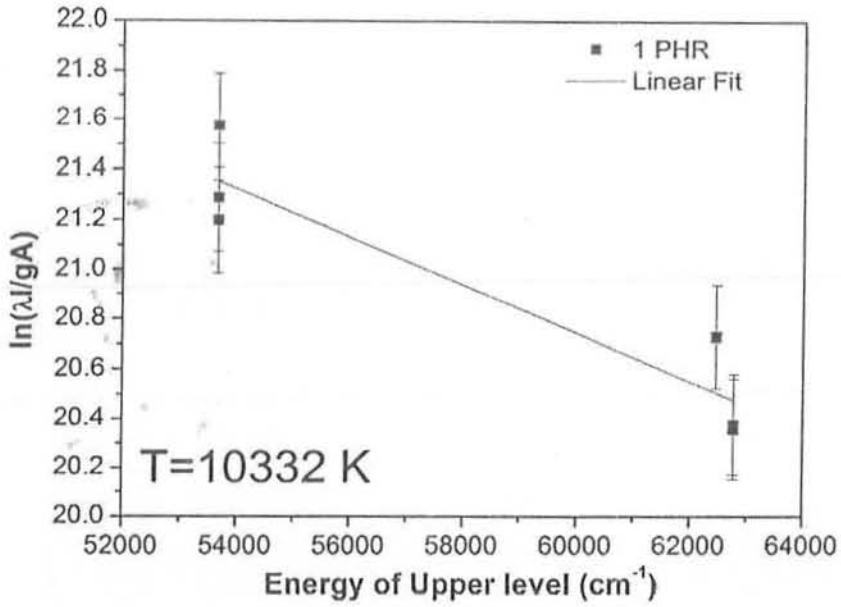

Fig 5 (b): *Typical Boltzmann-Plot. Emission lines from neutral Zn of sample B are used for obtaining temperature.*

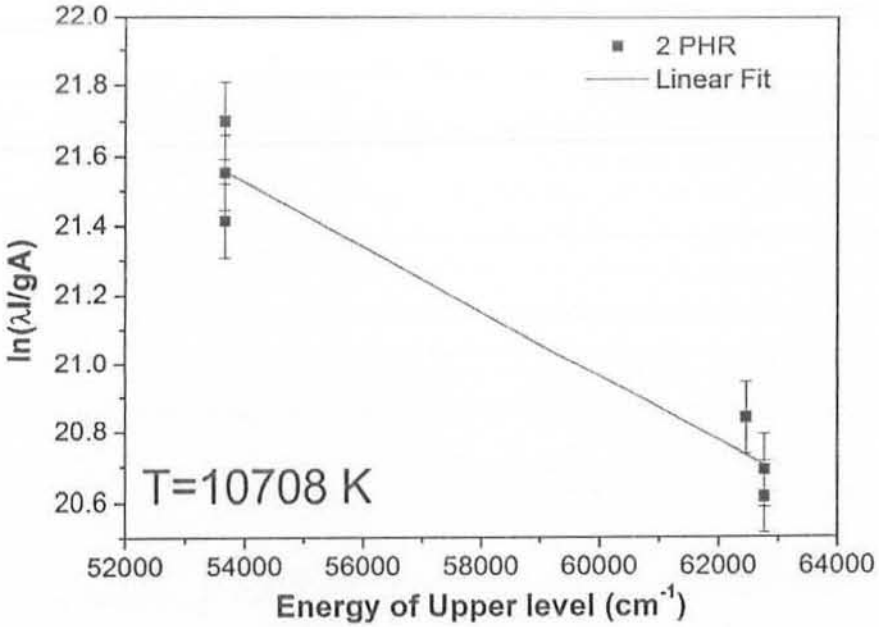

Fig 5 (c): *Typical Boltzmann-Plot for estimating the plasma Temperature. Emission lines from neutral Zn of sample C are used for obtaining temperature.*

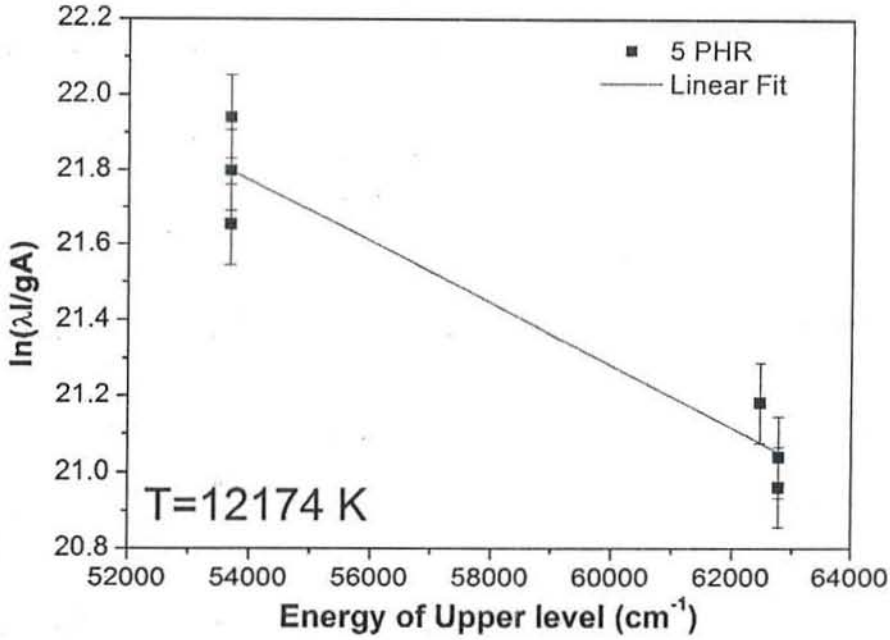

Fig 5 (d): *Typical Boltzmann-Plot for estimating the plasma Temperature. Emission lines from neutral Zn of sample D are used for obtaining temperature.*

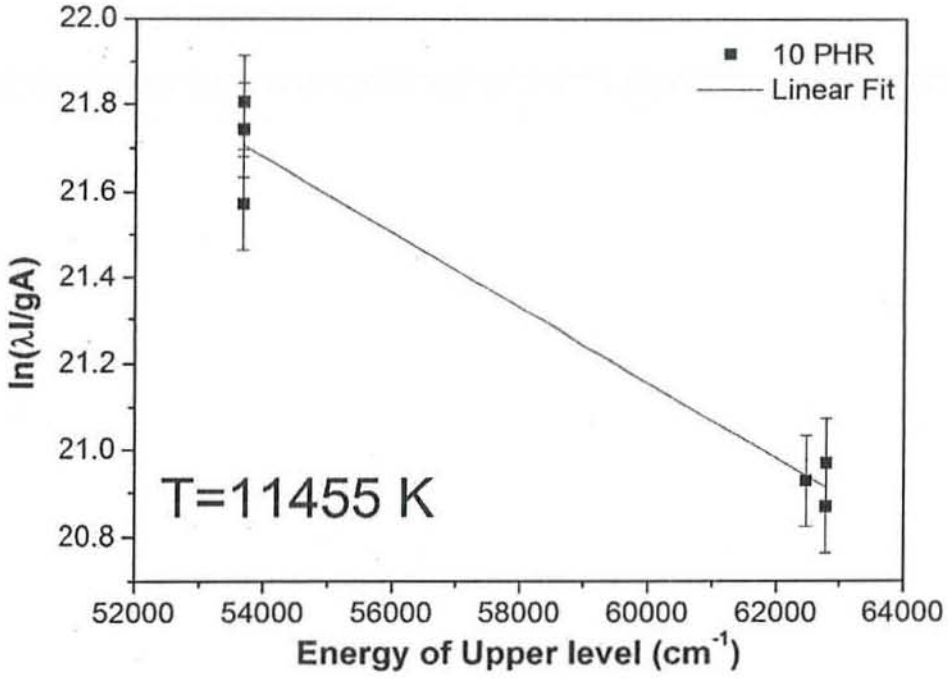

Fig 5 (e): *Typical Boltzmann-Plot for estimating the plasma Temperature. Emission lines from neutral Zn of sample E are used for obtaining temperature.*

Temperatures obtained from Al plots and Zn plots vary with each other. To minimize the statistical errors, average is taken of both temperatures for each sample. Average temperature is used further in quantitative analysis. All temperatures and averages are tabulated below:

Table 4: Temperatures from Boltzmann Plots and their averages

Samples /Temp	Temp from Zn lines (K)	Temp from Al lines (K)	Mean Temperature (K)
Sample A	11352	17079	14215.5
Sample B	10332	12437	11384.5
Sample C	10708	11290	10999
Sample D	12174	12710	12442
Sample E	11455	11940	11698

2.2 Calculation of Electron Number Density (N_e)

Electron Number Density is calculated by Stark broadening parameter. We have selected different spectral lines for the calculation of N_e. FWHM is calculated for each peak by Lorentzian fit. By using the formula mentioned in Eq. 3.14, N_e is calculated. Calculated number densities and their averages values are tabulated in Table 4.3.

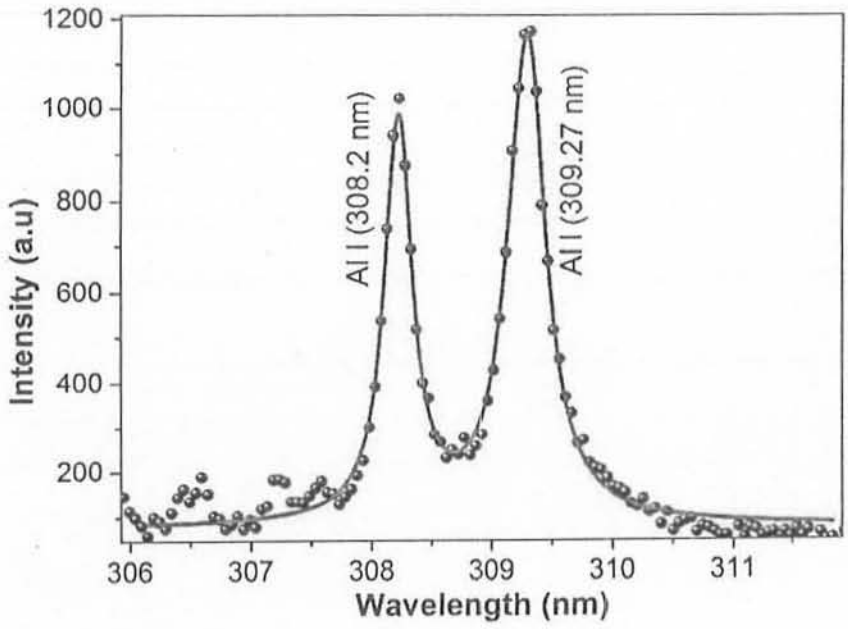

Fig 3 (a): Lorentzian double fit for Al (I) lines (308.2nm and 309.2 nm) of sample E

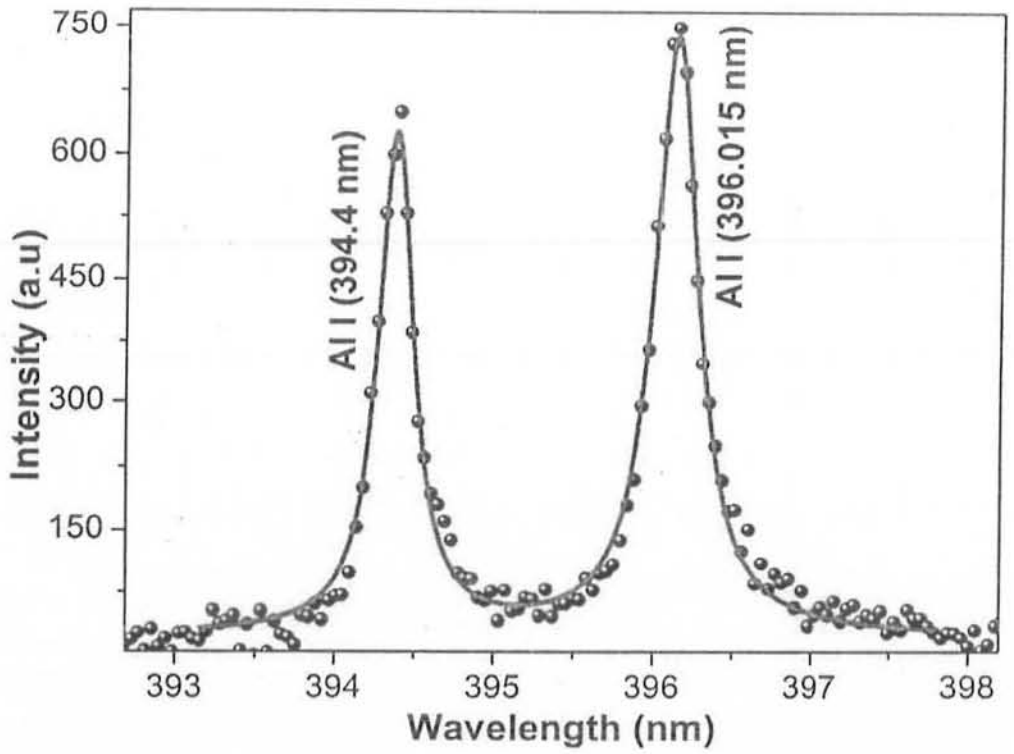

Fig 3 (b): Lorentzian double fit for Al (I) lines (394.4 nm and 396.15 nm) of sample E

Table 3: *Electron densities of different peaks and their averages (10^{17} cm^{-3})*

Peaks/ Samples	A (0.5 PHR)	B (1 PHR)	C (2 PHR)	D (5 PHR)	E (10 PHR)
394.36	0.280338	0.714894	1.29206	1.04734	2.10083
396.11	0.210251	0.964479	1.60834	1.55541	2.92422
308.22	0.979504	1.11384	2.17977	1.17963	2.16604
309.27	0.675627	1.26599	3.19621	1.41758	3.02711
Average	0.53643	1.0148	2.0691	1.29999	2.55455

2.3 Pre-requisites for analysis

2.3.1 Local Thermodynamic Equilibrium:

It is a check to confirm that excitation and de-excitation all occurs at the same temperature. A criterion is set on the electron number density, which is:

$$N_e \geq 1.6 \times 10^{12} T^{\frac{1}{2}} (\Delta E)^3 \qquad (4.1)$$

Here ΔE is the difference of energy of upper and lower levels in eV and T is temperature in Kelvin. We check LTE condition for Al 394.4 nm. For this line,

$\Delta E = 3.1291$ eV

T=14215.5 K (maximum recorded temperature)

Thus, upper bound on the N_e will be:

$N_e = 5.8 \times 10^{15}\ cm^{-3}$

Our estimated values of N_e are in $10^{17}\ cm^{-3}$ (Table 4.3) which is much greater than value obtained from the above inequality ($10^{15}\ cm^{-3}$). Hence, it can be said with surety that the plasma satisfies this condition.

2.3.2 Validity of Optically Thin Plasma:

This is another required condition. It is checked by comparing intensity ratio of two spectral lines and comparing it with theoretical values.

Spectral lines tabulated in Table 4.1 fulfil the criteria for optically thin plasma. This is ensured by comparing theoretical and experimental values close to each other. In order to minimize the dependence on plasma temperature, ratio is taken for the lines having close upper energy levels.

Ratios of pairs of spectral lines along with their intensities along with their theoretical and experimental values are tabulated in Table 4.4. These ratios are comparable for all spectral lines.

Table 4: *Comparison of experimental and theoretical ratios for spectral lines for sample A*

Pairs	Wavelength (nm)	Intensity (a.u)	Theoretical ratio	Experimental ratio
Al				
1	257.5	87.25	3.33	3.15
	308.2	229.19		
2	308.2	229.19	0.54	0.66
	309.27	274.77		
3	394.4	111.27	0.51	0.75
	396.15	169.3		

2	330.258 334.51	1226.0 1316.09	1.02	0.96
3	468.015 472.215	914.35 1700.72	0.81	0.72
4	468.015 481.053	914.35 3132.02	0.54	0.40

Since the above two conditions have been checked, we can proceed to CF LIBS procedure.

2.4 Compositional Analysis

Concentration are estimated by calculating number density n of excited atoms by neutral and spectral lines from ions. Number density n of neutral lines is calculated by the relation 3.12. It is possible to plot a Boltzmann plot for neutral lines most of the times. So, by using plasma parameters (mainly temperature from the plot) one can reach to the concentration.

Ionic lines, the spectral lines from ions, are tricky to deal with. If a Boltzmann can be drawn for ionic lines, we are in a position to define its temperature. In the present case, it was impossible to plot a reliable Boltzmann plot for these lines due to their fewer number and much reduced intensities. So, Saha-Boltzmann Equation (Eq. 3.13) was used. This equation is basically ratio between number densities from neutral as well as lines from ions, so if one is known, we can get the other.

3 Energy Dispersive X rays Spectroscopic (EDX) Analysis

In EDX, energetic beam of electrons imping on the sample knocking out inner shell electrons leaving a vacant site. These vacancies are filled by higher level electrons emitting photons of characteristic energies. Concentration of element is determined by measuring number of photons thus emitted.

In Fig 4.6, energies of photons (keV) are plotted against the number of photons (arbitrary units). By measuring heights of the peaks against the characteristic energies, compositional analysis is carried out. EDX is carried out by the SEM with attached EDX setup.

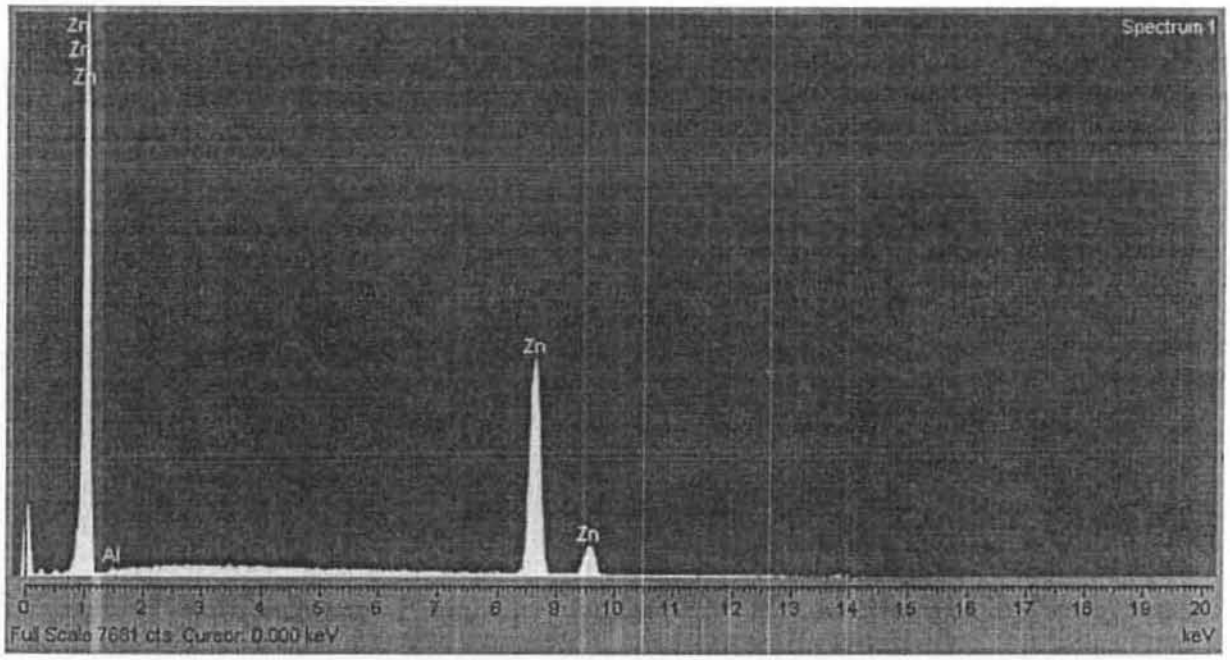

Fig 6 (a): EDX Spectrum of Sample A

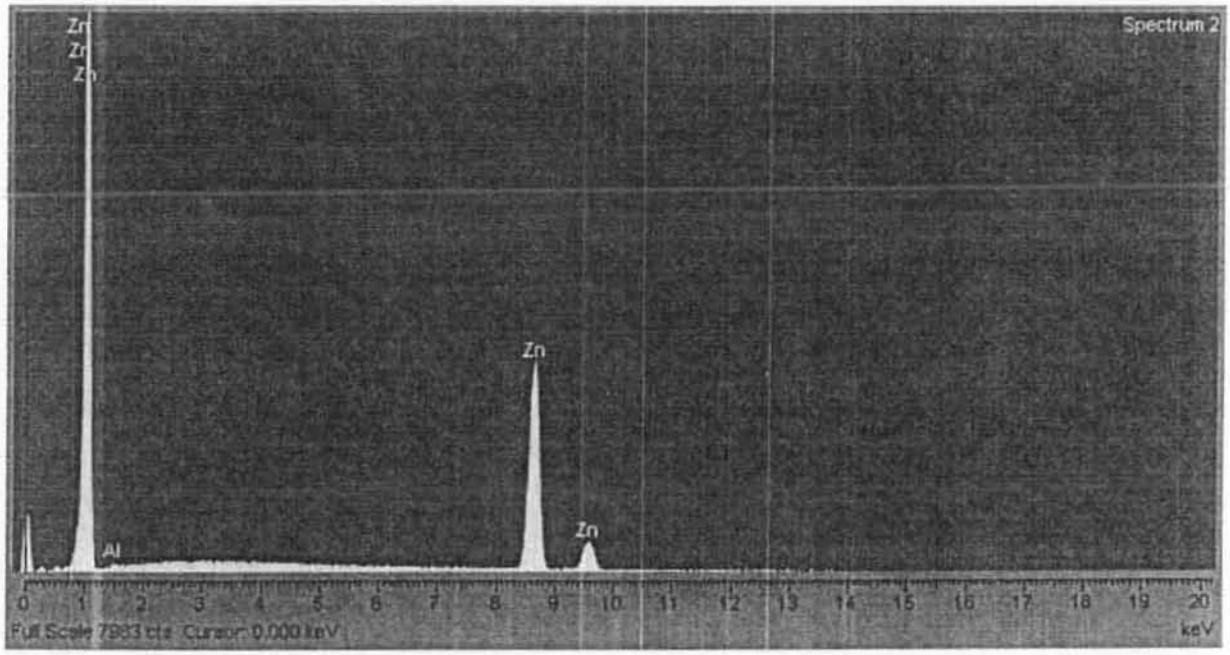

Fig 6 (b): EDX Spectrum of Sample B

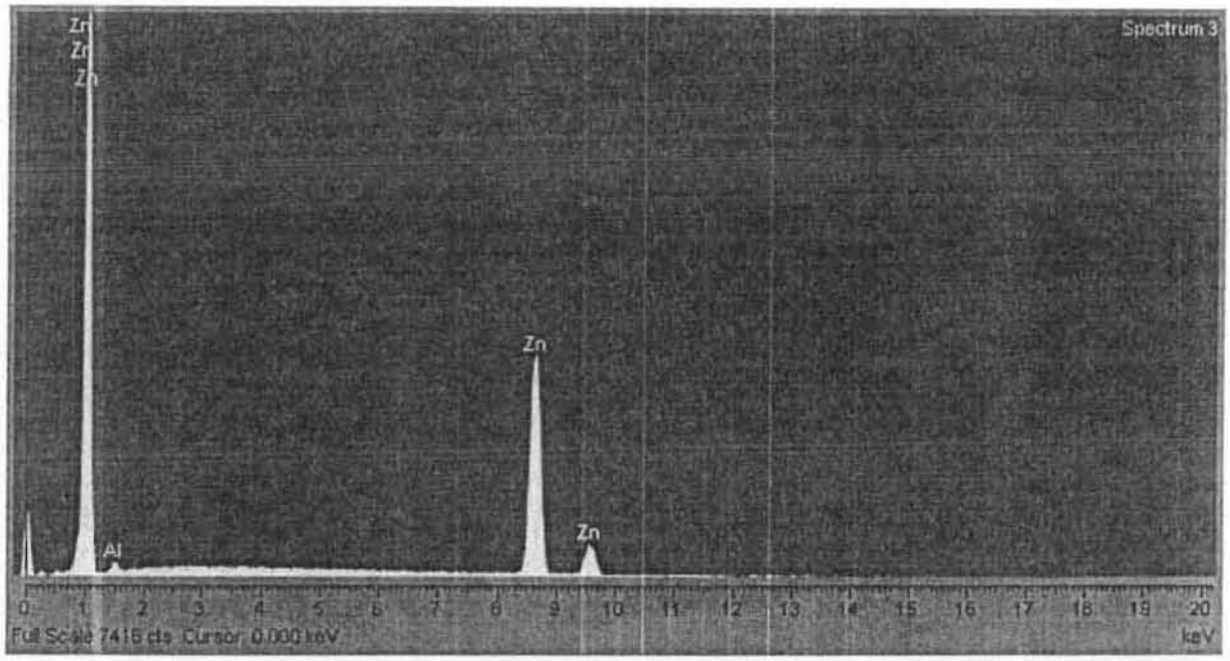

Fig 6 (c): EDX Spectrum of Sample C

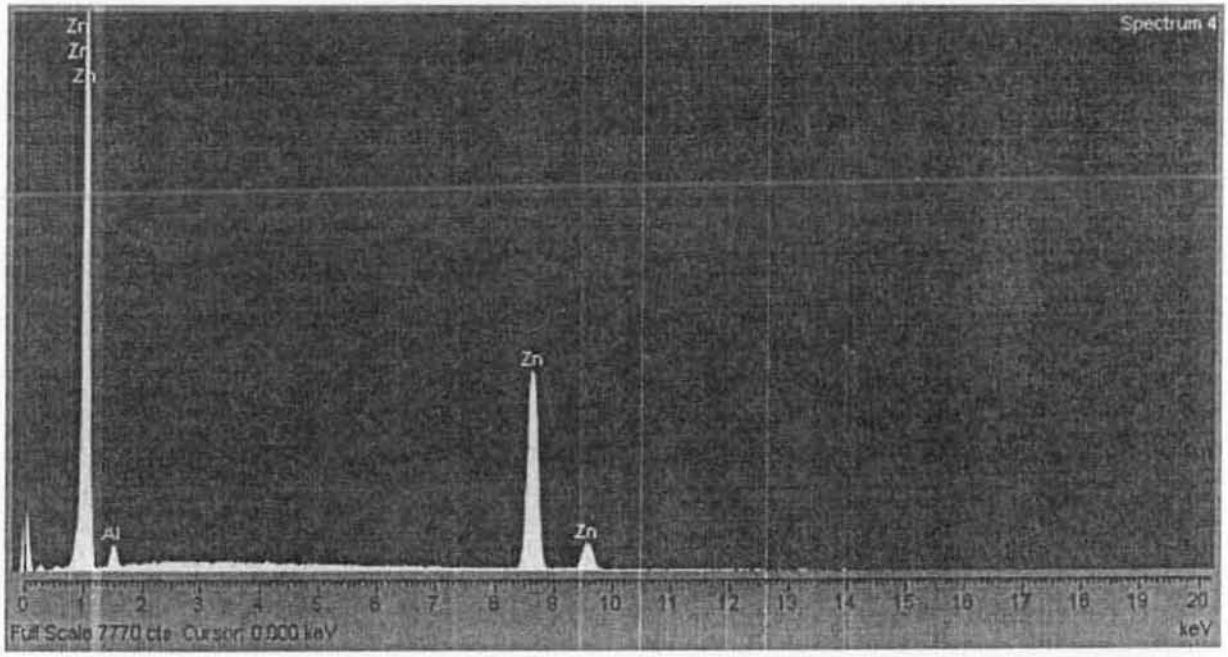

Fig 6 (d): EDX Spectrum of Sample D

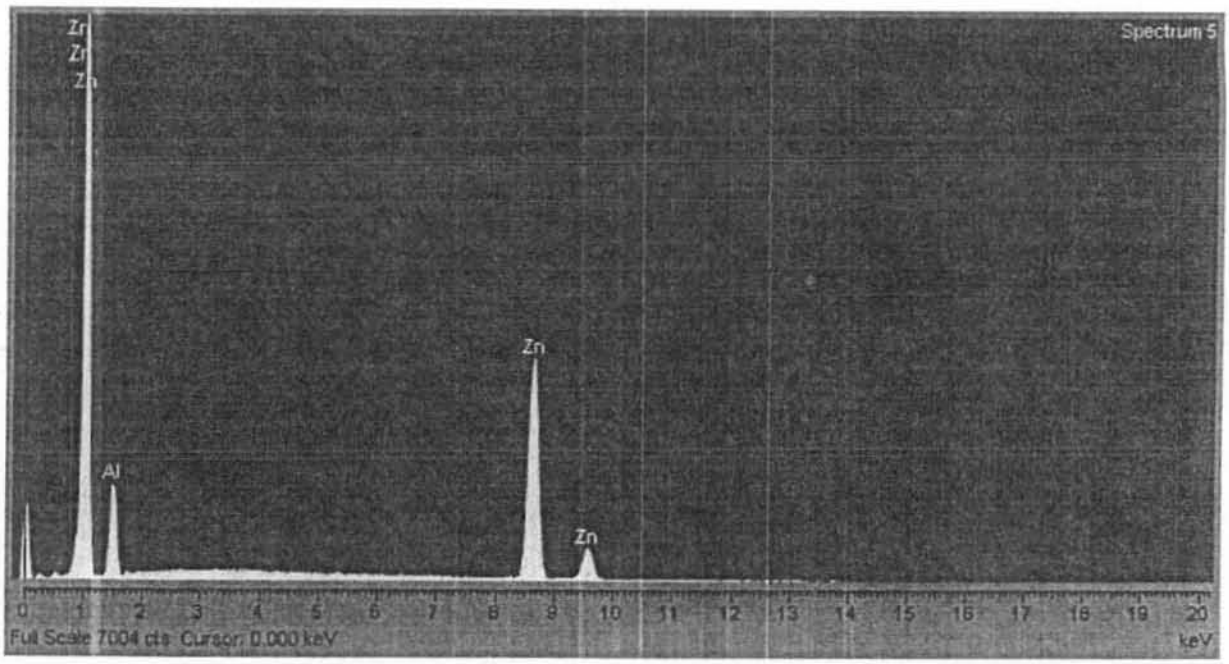

Fig 6 (e): EDX Spectrum of Sample E

We took five different reading by zooming to different areas on the sample. By this more confidence is achieved for our readings as statistical errors are minimized. This method is very suitable for the samples having the chance of inhomogeneity as in this case.

Table 5: *Compositional analysis with EDX and their averages*

Sample Alphabet	Percentage prepared Al (%)	Reading 1 Al (%)	Reading 2 Al (%)	Reading 3 Al (%)	Reading 4 Al (%)	Reading 5 Al (%)	Average Result Al (%)
A	0.5	0.36	0.20	0.53	-	-	0.36
B	1	0.77	0.39	0.51	0.40	0.57	0.53
C	2	0.87	0.91	1.10	1.05	1.12	1.01
D	5	1.86	2.28	3.49	3.00	2.85	2.70
E	10	7.75	9.26	13.09	9.64	9.85	9.92

4 Comparison of LIBS based techniques with EDX and XRF

From Table 4.6, it is evident that the samples are inhomogeneous. Since, powders of both metals are mixed together, there is a considerable chance of inhomogeneity. Moreover, a small area is under consideration in EDX as compared to XRF, so its results deviates more from actual except for the last sample which may be due to some other error.

As for LIBS, large errors are present for low concentrations. But on increasing the concentration, it becomes less deviating. Thus, it can be assured that use of CF-LIBS method is fruitful only for samples having five percent or higher concentration. For low concentration, CC method is more accurate and reliable.

Table 6: *Comparison with EDX and XRF with LIBS*

Samples	Prepared		XRF		EDS		LIBS	
	Al (%)	Zn (%)	Al (%)	Zn (%)	Al (%)	Zn (%)	Al (%)	Zn (%)
A	0.49	99.51	0.33	99.67	0.36	99.64	1.77	98.23
B	0.99	99.01	0.77	99.23	0.53	99.47	3.13	96.87
C	1.96	98.04	1.32	98.68	1.01	98.99	3.31	96.69
D	4.76	95.24	4.73	95.27	2.70	97.30	3.55	96.45
E	9.09	90.91	14.5	85.5	9.92	90.08	7.62	92.38

5 Conclusion

We have performed quantitative analysis of Zn-Al alloy with varying concentration of Al and Zn, where Zn is used as a base element. Two LIBS based techniques, namely calibration free laser induced breakdown spectroscopy and calibration curve method, are employed for compositional analysis. This study suggests that calibration curve method is a good option but reference samples are needed for drawing calibration curves between the emission lines intensities versus known compositions. The composition of the unknown samples can be estimated by comparing the emission line intensity from the calibration curves. Good linear behaviour of the calibration curve suggests a good analysis. Any similar sample can be easily analysed by matching its intensity in the graph. Furthermore, limit of detection can be easily calculated from the curve.

Calibration Free CF-LIBS method provides good elemental composition for high concentration samples. This technique gives more accurate results when concentration was above two percent, but for low concentrations results are not so good.

References

[1] J. Wilson, J.F.B. Hawkes, Principles and Applications of Lasers, Prentice Hall Publications, ISBN (1987) 013523697-5.

[2] D.C. O'Shea, W.R. Callen, W.T. Rhodes, Introduction to Lasers and Their Applications, Addison-Wesley, London, 1978.

[3] T. H. Maiman. Stimulated optical radiation in ruby, Nature, 187 (4736) (1960) 493–494.

[4] T.H. Maiman, V. Evtuhov, R.H. Hoskins, I.J. Dhaenens, C.K. Asawa, Stimulated optical emission in fluorescent solids, spectroscopy and stimulated emission in ruby, Phys. Rev, 123(4) (1961) 1151-57.

[5] J.E. Geusic, H.M. Marcos, L.G. Van Uitert, Laser oscillations in Nd-doped yttrium aluminum, yttrium gallium, and gadolinium garnets, App. Phys. Lett. 4 (1964) 182–184.

[6] O. Svelto, Principles of Lasers, Plenum Press New York, 1989

[7] F. Brech, L. Cross, Optical micro emission stimulated by a ruby laser, Appl. Spectrosc, 16 (1962) 59.

[8] J. P. Singh, S. N. Thakur, Laser-Induced Breakdown Spectroscopy, Elsevier, 2007.

[9] R. J. Goldston, P. H. Rutherford, Introduction to Plasma Physics, Institute of Physics Publishing LTD, Philadelphia, PA, 1995.

[10] A. W. Miziolek, V. Palleschi, I. Schechter, Laser-Induced Breakdown Spectroscopy (LIBS), Fundamentals and Applications, Cambridge University Press, New York, 2006.

[11] J. Bengoechea, C. Aragon, J.A. Aguilera, Asymmetric Stark broadening of the FeI 538.34 nm emission line in a laser induced plasma, Spectrochimica Acta Part B 60 (2005) 897 – 904.

[12] J. Bengoechea, J.A. Aguilera, C. Aragon, Application of laser-induced plasma spectroscopy to the measurement of Stark broadening parameters, Spectrochimica Acta Part B 61 (2006) 69 – 80.

[13] T. Ctvrtnickova, L. Cabalin, J. Laserna, V. Kanicky, G. Nicolas, Laser ablation of powdered samples and analysis by means of laser-induced breakdown spectroscopy, Applied Surface Science 255 (2009) 5329–5333.

[14] M. Hanif, M. Salik, M. A. Baig, Diagnostic Study of Nickel Plasma Produced by Fundamental (1064 nm) and Second Harmonics (532 nm) of an Nd: YAG Laser, Journal of Modern Physics, 3 (2012) 1663-1669.

[15] C. Gautier, P. Fichet, D. Menut, J. Dubessy, Applications of the double-pulse LIBS in the collinear beam geometry to the elemental analysis of different material, Spectrochimica Acta Part B 61 (2006) 210–219.

[16] V. Lazic, R. Barbini, F. Colao, R. Fantoni, A. Palucci, Self-absorption model in quantitative laser induced breakdown spectroscopy measurements on soils and sediments, Spectrochimica Acta Part B 56 (2001) 807-820

[17] A.M.E. Sherbini, T.M.E Sherbini, H. Hegazy, G. Cristoforetti, S. Legnaioli, V. Palleschi, L. Pardini, A. Salvetti, E. Tognoni, Evaluation of self-absorption coefficients of aluminum emission lines in laser-induced breakdown spectroscopy measurements, Spectrochimica Acta Part B 60 (2005) 1573 – 1579.

[18] P. Stavropoulos, C. Palagas, G.N. Angelopoulos, D.N. Papamantellos, S. Couris, Calibration measurements in laser-induced breakdown spectroscopy using nanosecond and picosecond lasers, Spectrochim. Acta Part B 59 (2004) 1885–1892

[19] G. Cristoforetti, G. Lorenzetti, S. Legnaioli, V. Palleschi, Investigation on the role of air in the dynamical evolution and thermodynamic state of a laser-induced aluminium plasma by spatial- and time-resolved spectroscopy, Spectrochim. Acta Part B 65 (2010) 787–796

[20] J.B. Simeonsson, A.W. Miziolek, Spectroscopic studies of laser-produced plasmas formed in CO and CO2 using 193, 266, 355, 532 and 1064 nm laser radiation, Appl. Phys. B 59 (1994) 1–9.

[21] G. Cristoforetti, A. De Giacomo, M. Dell'Aglio, S. Legnaioli, E. Tognoni, V. Palleschi, N. Omenetto, Local thermodynamic equilibrium in laser-induced breakdown spectroscopy beyond the McWhirter criterion, Spectrochim. Acta Part B 65 (2010) 86–95.

[22] D.W. Hahn, N. Omenetto, Laser-induced breakdown spectroscopy (LIBS), part I: review of basic diagnostics and plasma–particle interactions: still-challenging issues within the analytical plasma community, Appl. Spectrosc. 64 (2010) 335A–366A.

[23] Marwa A. Ismail, Hisham Imam, Asmaa Elhassan, Walid T. Youniss and Mohamed A. Harith, LIBS limit of detection and plasma parameters of some elements in two different metallic matrices, J. Anal. At. Spectrom. , 19 (2004) 489 –494

[24] D.A. Cremers and L.J. Radziemski, Hand book of Laser Induced Breakdown Spectroscopy, Wiley, New York, 2007.

[25] G. Bekefi, Principles of Laser Plasma, Wiley, New York, 1976.

[26] M.A. Gigosos, M.A. Gonzalez, V. Cardenoso, Computer simulated Balmer-alpha, -beta and -gamma Stark line profiles for non-equilibrium plasmas diagnostics, Spectrochimica Acta Part B 58 (2003) 1489–1504.

[27] S. S. Harilal, Beau O''Shay, Yezheng Tao, and Mark S. Tillack J. Appl. Phys. 99, 083303 (2006).

[28] N. Farid, S. Bashir and K. Mahmood Phys. Scr. 85 015702 (7pp) (2012).

[29] Muhammad Musadiq, Nasir Amina, Yasir Jamila, Munawar Iqbalb, M. Asif Naeema and Hafiz Akif Shahzada, Measurement of electron number density and electron temperature of laser-induced silver plasma.

[30] M. Hanif, M. Salik, M. A. Baig, Laser Based Optical Emission Studies of Zinc Oxide (ZnO) Plasma Received: 12 May 2013/Accepted: 9 August 2013/Published online: 23 August 2013.

[31] A. Bogaerts, Z. Chen Spectrochimica Acta Part B 60 1280 – 1307 (2005).

[32] M. Crank, S. S. Harilal, S. M. Hassan, and A. Hassanein Journal of Applied Physics 111, 033301 (2012).

[33] S. S. Harilal, R. W. Coons, P. Hough, and A. Hassanein Applied Physics Letters 95, 221501 (2009).

[34] S. S. Harilal Journal of Applied Physics 102, 123306 (2007)

[35] Y. Ueno, G. Soumagne, A. Sumitani, A. Endo, and T. Higashiguchi, Appl. Phys. Lett. 91, 231501 (2007)

[36] S. S.Harilal, T. Sizyuk, V. Sizyuk, and A. Hassanein, Appl. Phys. Lett. 96, 111503 (2010).

[37] M. Hanif, M. Salika, M.A. Baig, Quantitative studies of copper plasma using laser induced breakdown spectroscopy.

[38] L.Z. Wu, R.Q. Shen, J. Xu, Y.H. Ye, Y. Hu, Spectroscopic study of laser-induced cu plasma with and without the confinement of a substrate, IEEE Trans. Plasma Sci. 38 (2010) 174–180.

[39] A. Sarkar, R.V. Shah, D. Alamelu, S.K. Aggarwal, Studies on the ns-IR-laser-induced plasma parameters in the vanadium oxide, J. At. Mol. Phys. 2011 (2011) 504764.

[40] J. White, P. Dunne, P. Hayden, F. O"Reilly, and G. O"Sullivan Applied Physics 90, 181502 (2007).

[41] J.E. Carranza, B.T. Fisher, G.D. Yoder, D.W. Hahn, On-line Analysis of Ambient Air Aerosols using Laser-induced Breakdown Spectroscopy, Spectrochim. Acta Part B 56 (2001) 851-864.

[42] B.C. Windom, P.K. Diwakar, D.W. Hahn, Dual-Pulse Laser Induced Breakdown Spectroscopy for Analysis of Gaseous and Aerosol Systems: Plasma-Analyte Interactions, Spectrochim. Acta Part B 61 (2006) 788-796.

[43] V. Juve, R. Portelli, M. Boueri, Y.J. Baudelet, Space-resolved Analysis of Trace Elements in Fresh Vegetables using Ultraviolet Nanosecond Laser-induced Breakdown Spectroscopy, Spectrochim. Acta Part B 63 (2008) 1047-1053.

[44] W. Lei, V. M. Ros, M. Boueri, Q. Ma, D. Zhang, L. Zheng, H. Zeng, J. Yu, Time-resolved Characterization of Laser-induced Plasma from Fresh Potatoes. Spectrochim. Acta Part B 64 (2009) 891-898.

[45] A. I. Whitehouse, J. Young, I. M. Botheroyd, S. Lawson, C. P. Evans, J. Wright, Remote material analysis of nuclear power station steam generator tubes by laser induced breakdown spectroscopy, Spectrochim. Acta Part B 56 (2001) 821–830.

[46] J. D. Winefordner, I. B. Gornushkin, T. Correll, E. Gibb, B. W. Smith and N. Omenetto, Comparing several atomic spectrometric methods, J. Anal. At. Spectrom. 19 (2004) 1061-1083.

[47] G. Cristoforetti, S. Legnaioli, V. Palleschi, A. Salvetti, E. Tognoni, P. A. Benedetti, F. Brioschi and F. Ferrario, Quantitative analysis of aluminium alloys, J. Anal. At. Spectrom. 21 (2006) 697-702.

[48] G. P.Gupta, B. M. Suri, A. Verma, M. Sunderaraman, V. K. Unnikrishnan, K. Alti, V. B. Kartha, C. Santhosh, Quantitative elemental analysis of nickel alloys using calibration-based laser-induced breakdown spectroscopy, J. Alloys Compd. 509 (2011) 3740-3745.

[49] B. Rashid, R. Ahmed, R. Ali, M.A. Baig, A comparative study of single and double pulse of laser induced breakdown spectroscopy of silver, Physics of Plasmas 18 (2011) 073301-073307.

[50] R. Ahmed, M. A. Baig, A comparative study of enhanced emission in double pulse laser induced breakdown spectroscopy, Opt. Laser Tech. 65 (2015) 113-118.

[51] J.A. Hernández, L.E.G. Ayuso, J.M.F. Romero, M.D.L.D. Castro, Partial Least Squares Regression for Problem Solving in Precious Metal Analysis by Laser Induced Breakdown Spectrometry. J. Anal. At. Spectrom. 15 (2000) 587-593.

[52] J.B. Sirven, B. Bousquet, L. Canioni, L. Sarger, Laser-induced Breakdown Spectroscopy of Composite Samples, Comparison of Advanced Chemometrics Methods, Anal. Chem. 78 (2006) 1462-1469.

[53] N.M. Shaikh, B. Rashid, S. Hafeez, Y. Jamil, M.A. Baig, Measurement of electron density and temperature of a laser-induced zinc plasma, J. Phys. D. Appl. Phys. 39 (2006) 1384–1391.

[54] B. Rashid, S. Hafeez, N.M. Shaikh, M. Saleem, R. Ali, M.A. Baig, Diagnostics of copper plasma produced by the fundamental, second and third harmonics of a Nd:Yag laser, Int. J. Mod. Phys. B 21 (2007) 2697–2710.

[55] M. Salik, M. Hanif, M.A. Baig, Plasma diagnostic study of alumina (Al2O3) generated by the fundamental and second harmonics of a Nd:YAG laser, IEEE Trans. Plasma Sci. 39 (2011) 1861–1867.

[56] M. Hanif, M. Salik, M.A. Baig, Optical spectroscopic studies of titanium plasma produced by an Nd:YAG laser, Opt. Spectrosc. 114 (2013) 7–14.

[57] D.A. Cremers and L.J. Radziemski, Hand book of Laser Induced Breakdown Spectroscopy, Joh Wiley & Sons Ltd, West Sussex, 2006.

[58] A. Ciucci, M. Corsi, V. Palleschi, S. Rastelli, A.Salvetti and E. Tognoni, New procedure for quantitative elemental analysis by laser-induced plasma spectroscopy, Appl. Spectrosc. 53 (1999) 960-964.

[59] E. Tognoni, G. Cristoforetti, S. Legnaioli, V. Palleschi, A. Salvetti, M. Mueller, U. Panne, I. Gornushkin, A numerical study of expected accuracy and precision in calibration- free laser-induced breakdown spectroscopy in the assumption of ideal analytical plasma, Spectrochim. Acta Part B 62 (2007) 1287-1302.

[60] R. Gaudiuso , M. Dell'Aglio, O. De Pascale, S. Loperfido, A. Mangone, A. De'Giacomo, Laser-induced breakdown spectroscopy of archaeological findings with calibration-free inverse method: Comparison with classical laser-induced breakdown spectroscopy and conventional techniques, Anal. Chimica Acta 813 (2014) 15-24.

[61] P. J. Kalmhofer, S. Eschlbock-Fuchs, N. Huber, R.Rossler, J. Heitz, J. D. Pedaening, Calibration-free analysis of steel slag by laser-induced breakdown spectroscopy with combined UV and VIS spectra, Spectrochim. Acta Part B (2015) 67-74.

[62] J.M. Gomba, C. D. Angelo, D. Bertuccelli, G. Bertuccelli, Spectroscopic characterization of laser induced breakdown in aluminium-lithium alloy samples for quantitative determination of traces, Spectrochimica Acta Part B 56 (2001) 695-705.

[63] Lanxiang Sun, Haibin Yu. Correction of self-absorption effect in calibration free laser-induced breakdown spectroscopy by an internal reference method. 2009.

[64] M.R. Joseph, N. Xu, V. Majidi, Time-resolved emission characteristics and temperature profiles of laser-induced plasmas in helium, Spectrochim. Acta Part B 49 (1994) 89–103.

[65] M. Essien, L.J. Radziemsky, J. Sneddon, Detection of cadmium, lead and zinc in aerosols by laser-induced breakdown spectrometry, J. Anal. At. Spectrom. 3 (1988) 985–988.

[66] C. Aragón, F. Peñalba, J.A. Aguilera, Spatial characterization of laser induced plasmas: distributions of neutral atom and ion densities, Appl. Phys., A 79 (2004) 1145–1148.

[67] M. S. Dimitrijevic, S. Sahal-Brechot, Stark Broadening of AI I Spectral Lines, Physica Scripta. 49, (1994), 34-38

[68] N. Konjevic, M.S Dimitrijevic, W.L Wiese, Experimental Stark widths and shifts for spectral lines J. Phys. Chem. Ref. Data 13 (1984) 619-647

[69] J.A. Aguilera, C. Aragon, Multi-elemental Saha-Boltzmann and Boltzmann plots in laser-induced plasmas, Spectrochim. Acta Part B 62 (2007) 378-385.

[70] S. Yalcin, D.R. Crosley, G.P. Smith, G.W. Faris, Influence of ambient conditions on the laser air spark, Appl. Phys., B 68 (1999) 121–130.

[71] A. Alonso-Medina and C. Colo'n, Astrophys. J. 672, 1286 2008.

[72] G. Bekefi, Principles of Laser Plasma, Wiley, New York, 1976.

[73] H. R. Griem, Principles of plasma Spectroscopy, Cambridge University Press, 1997.

[74] W. Andrzej, V. Palleschi and S. Israel, Laser Induced Breakdown Spectroscopy (LIBS) fundamentals and applications, Cambridge University, New York, 2006.

[75] L.J. Radziemski, T.R. Loree, D.A. Cremers, N.M. Hoffman, Time resolved laser-induced breakdown spectrometry of aerosols, Anal. Chem. 55 (1983) 1246–1252.

[76] J.B. Simeonsson, A.W. Miziolek, Time-resolved emission studies of ArF-laser- produced micro plasmas, Appl. Opt. 32 (1993) 939–947.

[77] M. Mila´n, J.J. Laserna, Diagnostics of silicon plasmas produced by visible nanosecond laser ablation, Spectrochim. Acta Part B 56 (2001) 275–288.

[78] V. K. Unnikrishnan, K. Mridul, R. Nayak, K. Alti, V. B. Kartha, C. Santhosh, G. P. Gupta, Calibration-free laser-induced breakdown spectroscopy for quantitative elemental analysis of materials, Pramana-Journal of Phys. 79 (2012) 299-310.

[79] Lu Y-F, Tao Z-B and Hong M-H 1999 Japan. J. Appl. Phys. 38 2958.

[80] Atwee T, Aschke L and Kunze H-J 2000 J. Phys. D: Appl. Phys. 33 2263.

[81] Abdellatif G and Imam H 2002 Spectrochim. Acta B 57 1155.

[82] McWhirter RWP. In: Huddleston RH, Leonard SL, editors. Plasma diagnostic techniques. New York: Academic Press; 1965.

[83] Cremers DA, Radziemski LJ. Handbook of laser-induced breakdown spectroscopy. New York: Wiley; 2006

[84] Barthe ´lemy O, Margot J, Laville S, Vidal F, Chaker M, Johnston TW, et al. Appl Spectrosc 2005;59(4):529–36.

[85] S. S. Harilal, B. O'Shay and M. S. Tillah, Spectroscopic characterization of laser-induced tin plasma, J. Appl. Phys. 98 (2005) 0133061-0133067

[86] NIST Database

[87] Reader J, Corliss C H, Wiese W L and Marlin G A 1980 Wavelengths and transition probabilities for atoms and atomic ions, US Department of Commerce